Flood Storage Allocation Rules for Parallel Reservoirs

By

RUI HUI
B.S. (Tsinghua University, China) 2011

THESIS

Submitted in partial satisfaction of the requirements for the degree of

MASTER OF SCIENCE

In

Civil and Environmental Engineering

In the

OFFICE OF GRADUATE STUDIES

Of the

UNIVERSITY OF CALIFORNIA

DAVIS

Approved:

_____

Jay R. Lund, Chair

_____

Bassam Younis

_____

Samuel Sandoval Solis

Committee in Charge

2013

Abstract

Operating policies have been derived for reservoirs in series and in parallel for various objectives. However, little analysis has been done for flood operations of parallel reservoir. In a parallel reservoir system, inflows for each reservoir should be regulated together to reduce downstream peak flow and minimize flood damage. However, for different hydrograph shapes, corresponding flood storage volumes often differ for the same peak flow reductions. Meanwhile, it is often the case that flood storage volume is constrained by reservoir storage capacity during major flood operations. The term *Flood Storage Efficiency* (FSE) - peak flow reduction per unit storage for a given hydrograph - is introduced to mathematically represent these ideas. Given a total flood storage capacity available for allocation, the optimal flood storage allocation rules are derived in terms of FSE for reservoirs in parallel based on likely inflow hydrographs. Theoretically, if ideally operated, the first-order derivative of FSE defined as the *marginal flood storage efficiency* (MFSE) of each parallel reservoir should be equalized. A deterministic model is developed for a single known storm and demonstrates the equal MFSE rule. Hydrograph effects are analyzed afterwards for typical conditions, including sensitivity to hydrograph shape. This model is then extended for an uncertain storm with probabilistic hydrograph, and a series of known and unknown storms. Similarly, ideal optimal operation rules for these complex models are to equalize all the MFSEs. Examples are given to illustrate the optimal results and different conditions are compared. Finally, the derived flood storage allocation rules are applied to flood operation of Oroville Reservoir and New Bullards Bar Reservoir in California's Sacramento River Basin with a single historical 1997 flood and an uncertain storm.

Keywords

Hydrograph shape, parallel reservoir, flood storage efficiency (FSE), marginal flood storage efficiency (MFSE), uncertainty.

Acknowledgements

I have worked with a couple of people who contributed a lot to the research and this thesis. I really appreciate their help in all aspects.

I would first like to thank my advisor, Jay Lund, for his guidance, advice, and supervision throughout my thesis. This thesis would not have been completed without his encouragement and effort. He also helped me get accustomed to life here in Davis. I am grateful to have him as an advisor and friend.

My thesis committee members, Bassam Younis and Samuel Sandoval Solis, have offered continued support and counsel throughout the writing of this thesis. Their knowledge and passion inspire me in my career.

During my daily study and research, I have received continuous support from other graduate students in my research group. I would like to thank all of them for their advice and suggestions. In particular, I would like to thank Prudentia Zikalala, Nathan Burley and James Connaughton for their comments and suggestions.

I would like to thank Brooke Noonan, Graduate Program Coordinator, and Amelia Brown, Student Affairs Officer, for their patience and responses to many emails throughout the submittal process.

Lastly, words cannot express my gratitude for my parents. I have been blessed with encouragement, support, guidance, and unconditional love throughout my entire life. I would not be where I am today without them. They are my role models and friends.

Table of contents

Tables

Figures

1. Introduction

The development and use of optimization techniques for planning, design, and management of complex water resources systems are longstanding in the field of water resources engineering (Yeh, 1985). A variety of common operating rules have been derived for single-purpose reservoirs in series and in parallel (Lund and Guzman, 1999). Labadie discusses the substantial technological challenges and rewards of integrated optimization of interconnected reservoir systems (Labadie, 2004). For multipurpose reservoirs, many approaches are available for flood season operation, for example the allocation of storage capacity for flood control based on explicit risk consideration (Jain et al. 1992), fuzzy rules (Shrestha, 1996), genetic algorithm (Chang, 2008) and dynamic programming (Kumar et al. 2010).

Flood management reservoirs regulate inflows to reduce downstream flood damages (Yazdi & Neyshabouri, 2012). During a flood, a reservoir stores some or all of the flood volume to reduce downstream peak flow. In Figure 1, a flood hydrograph is characterized by a rising limb, a recession limb, a peak inflow, duration of flood and duration of peak inflow. Ideally, a reservoir reduces the maximum outflow to the downstream channel capacity (dashed line), and the excess flow is stored in the reservoir for later release.

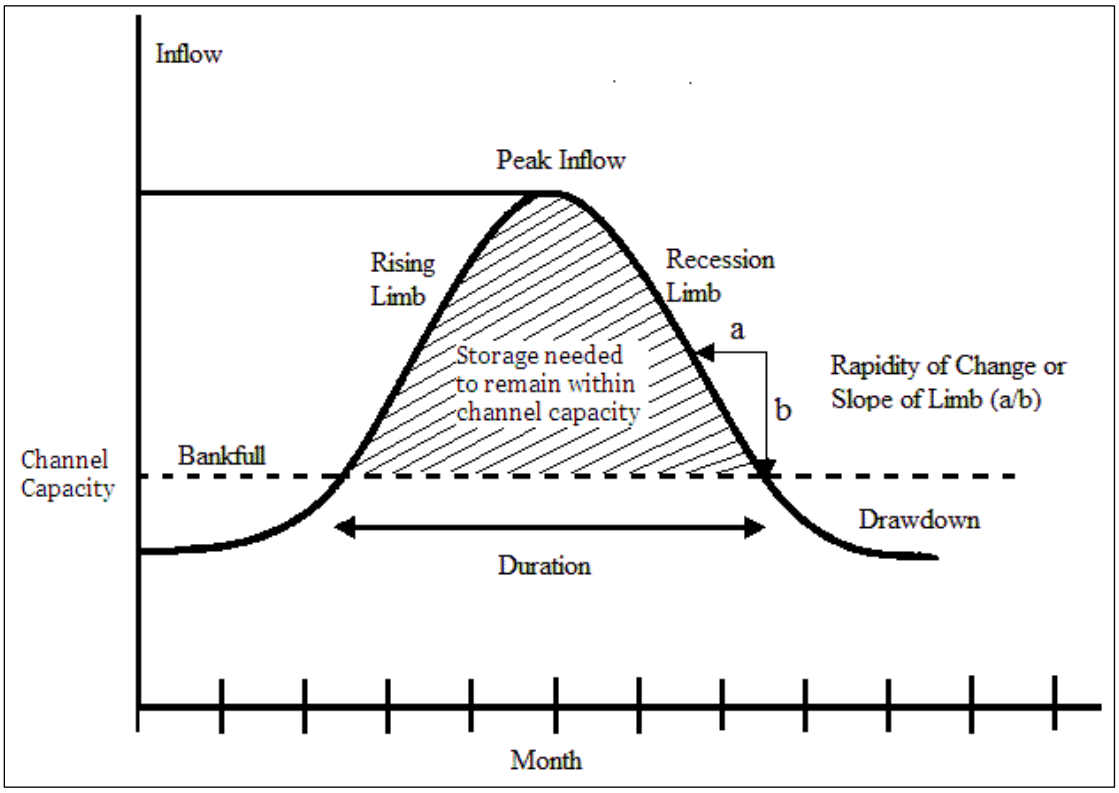

Figure 1. A typical flood hydrograph

This study shows how flood hydrograph shape drives optimization of flood operation for a system of parallel reservoirs. For a reservoir system operated for flood management, reservoirs are operated together to keep downstream flow below a given

channel capacity or to minimize peak downstream flow. Allocating flood storage capacity among parallel reservoirs is a complex problem. Factors, such as peak flow, duration of flood, shape and timing of hydrographs, reservoir storage capacity, outlet capacity, and downstream channel capacity influence ideal allocation. A complex stochastic multiobjective optimization method can find noninferior solutions for the operation of parallel reservoir (Wang et al. 2005). Maintaining a balance between reservoirs in terms of available storage capacities and expected flood runoff from drainage areas is one approach (Lund & Guzman, 1999). Consider two hydrograph shapes (Figure 2) with the same peak inflows (Figure 2, left) or the same flood volumes (Figure 2, right), for a given reduction of peak flow, the required flood storage volumes are quite different. However, it is always the case that flood storage volume constrains operation. So a question is raised that how available flood storage capacity be optimally allocated to minimize downstream damage.

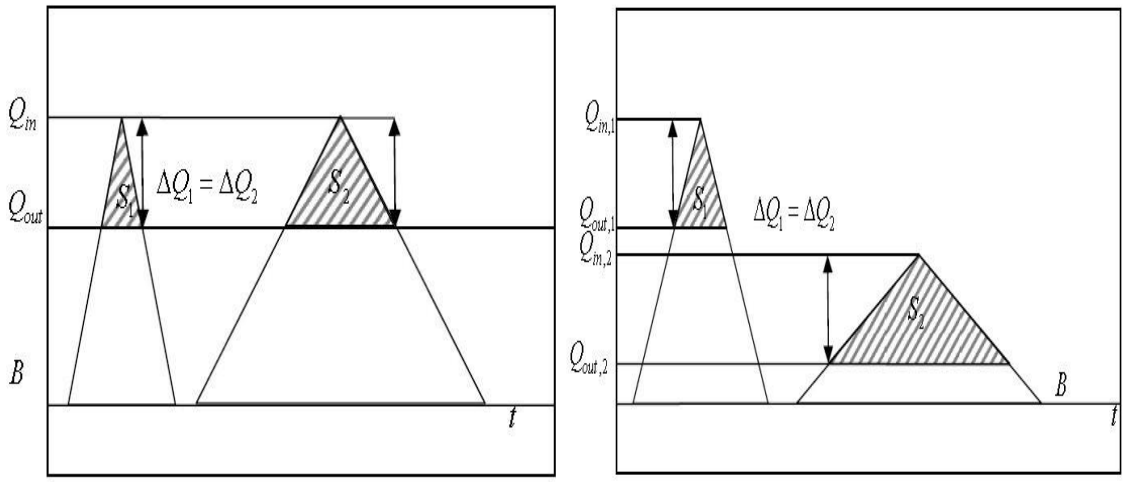

Figure 2. Constant peak flow reductions with different flood storage volumes for various paired hydrographs. Two hydrographs with the same peak inflow (left) or the same flood volume (right).

This thesis examines the effects of hydrograph shapes on optimal flood storage allocation rules for parallel reservoirs. Generalization of the relationship between peak flow reduction and flood storage volume for different hydrograph shapes is presented first. Two concepts for a hydrograph are defined: 1) *Flood Storage Efficiency* (FSE) is the peak flow reduction per unit flood storage volume; 2) *Marginal Flood Storage Efficiency* (MFSE) is the first-order derivative of FSE, representing changes of peak flow reduction with additional flood storage volume. Optimal flood storage allocation rules are derived for a simple deterministic case with a single known storm. The effects of various physical constraints (i.e. reservoir capacities, outflow reduction) and changes of allocations due to the ratio of *marginal flood storage efficiency* (MFSE) across reservoirs are analyzed. This process is then modified for uncertain storms, with complexity both from several floods sharing reservoir capacity together and the probabilities of each forecasted storm. To see how the derived optimal flood storage allocation rules work, these rules are applied to flood operation of Oroville Reservoir and New Bullards Bar Reservoirs in the Sacramento River Basin with historical flood records (basically the 1997 flood event) as a case study. The thesis concludes with discussions of limitations and conclusions.

2. Hydrograph Shape

Relative hydrograph size and shape are important for optimal flood storage allocations.

2.1 Generalized Hydrographs

Numerical modeling is done for the four basic hydrograph shapes in Figure 3: triangular, abrupt wave, flood pulse and broad peak. Each hydrograph shape has a peak inflow $Q_{i,inpeak}$, a rising limb and a recession limb a_i and b_i, and duration of the peak d_i. The other parameters here are peak outflow $Q_{i,outpeak}$, peak flow reduction ΔQ_i, flood storage volume S_i (the shaded area) and incoming flood volume (the total area). Hydrograph shape 1 has a simple triangular shape with linear rise and recession. Hydrograph shape 2 has an abrupt flood wave followed by a linear recession. Hydrograph shape 3 is a simple rectangular pulse. And hydrograph shape 4 is a more general trapezoid with an extended peak between the linear rise and recession. For simplification, assumptions are made that peak inflows occur at the same time, downstream travel time is uniform for outflow from each reservoir, no water loss and no peak attenuation occur along the stream.

To generate the relationship of peak flow reduction and flood storage volume for these four hydrograph shapes, we can simply use the two slopes of the inflow and duration of peak flow. The relationship of $Q_{i,inpeak}$, a_i , b_i , d_i , ΔQ_i , and S_i can be derived using the more general broad peak hydrographs shape. When $d_i = 0$ it becomes triangular hydrograph shape; when $d_i = 0$ and $a_i \to +\infty$ it becomes abrupt wave hydrograph shape; when $a_i \to +\infty$ and $b_i \to +\infty$ it becomes flood pulse hydrograph shape.

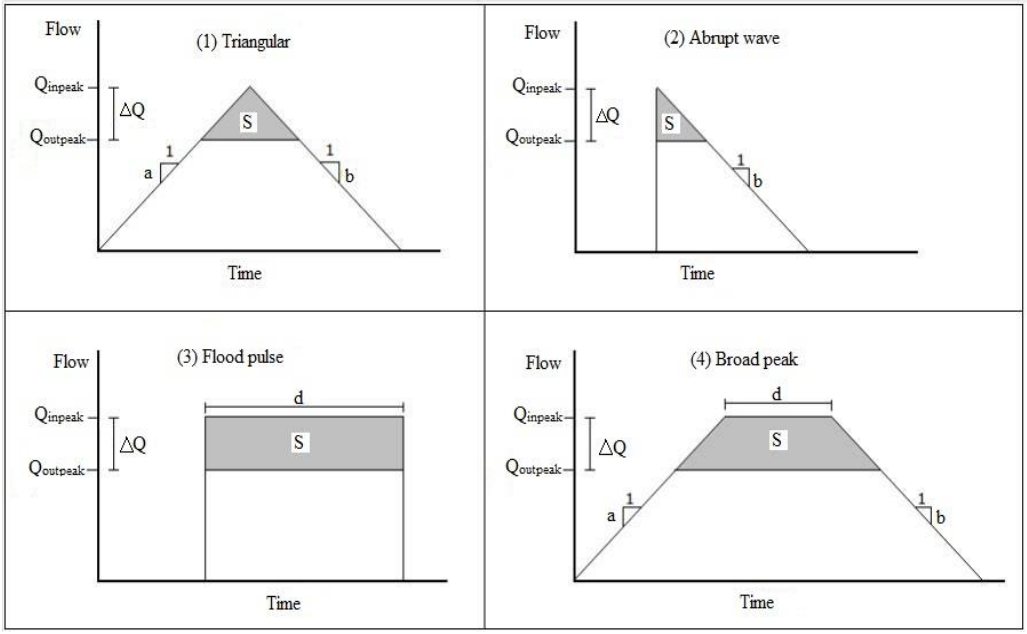

Figure 3. Four basic hydrograph shapes

Geometrically, the maximum ideal peak flow reduction from allocating flood storage S_i to reservoir *i*, is derived as follows:

$$S_i = \frac{\Delta Q_i}{2}\left(\frac{\Delta Q_i}{a_i} + \frac{\Delta Q_i}{b_i}\right) + d_i \Delta Q_i ,$$

$$\text{or } S_i = \frac{\Delta Q_i^{\,2}}{2}\left(\frac{1}{a_i} + \frac{1}{b_i}\right) + d_i \Delta Q_i ,$$

$$\text{or } S_i = \left(\frac{a_i + b_i}{2 a_i b_i}\right)\Delta Q_i^{\,2} + d_i \Delta Q_i , \qquad (1)$$

Using this quadratic equation to solve for maximum ΔQ_i:

$$\Delta Q_i = \frac{-d_i \pm \sqrt{d_i^{\,2} - 4 \times \left(\frac{a_i + b_i}{2 a_i b_i}\right) \times (-S_i)}}{2 \times \left(\frac{a_i + b_i}{2 a_i b_i}\right)} = \frac{-d_i + \sqrt{d_i^{\,2} + 2 S_i \left(\frac{a_i + b_i}{a_i b_i}\right)}}{\frac{a_i + b_i}{a_i b_i}} = \frac{-d_i + \sqrt{d_i^{\,2} + 2 \alpha_i S_i}}{\alpha_i} \qquad (2)$$

where

$$\alpha_i = \frac{a_i + b_i}{a_i b_i} .$$

Under the above simplified conditions, Equation (2) provides a general formula of peak reduction depending on flood storage.

2.2 Flood Storage Efficiency (FSE)

FSE can be explained with a simple hydrograph characterized by a rising limb, a recession limb and peak flow duration. As shown in Figure 4 (left), peak reduction is decreasing for additional flood storage volume. Correspondingly, on the right side of Figure 4, the accumulated peak flow reduction is a concave function of flood storage volume with a decreasing slope. For a typical flood hydrograph shape with ideal operation, accumulated peak flow reduction increases at a decreasing rate.

Conversely, the rate of increased flood storage volume for additional unit of increased peak flow reduction is increasing.

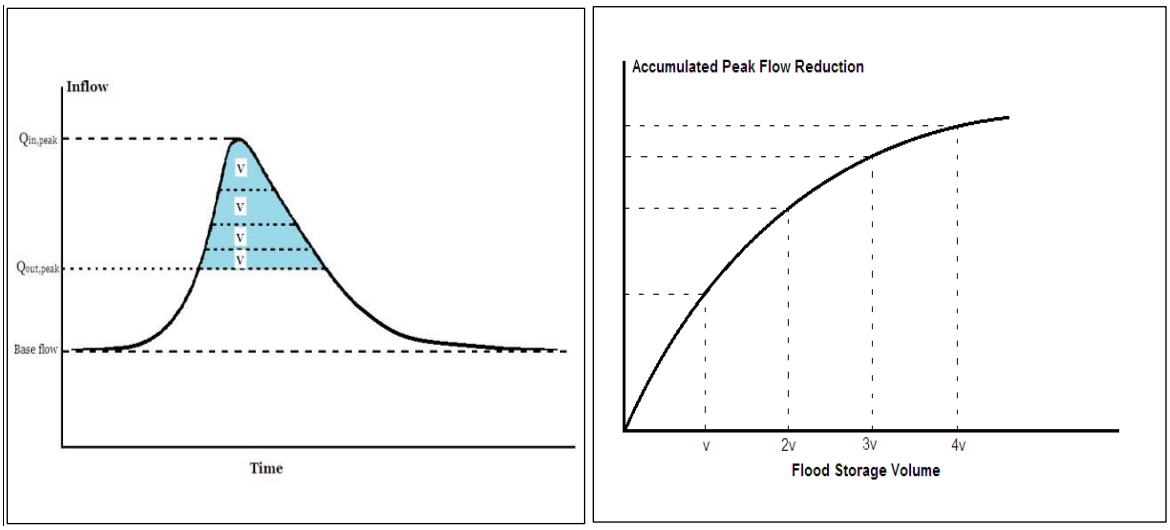

Figure 4. Increase of peak flow reduction with increasing flood storage volume

Flood Storage Efficiency (FSE) represents this relationship of peak flow reduction and flood storage volume for a given hydrograph shape. FSE is defined as peak reduction per unit flood storage (Equation (3)):

$$FSE_i = \frac{\Delta Q_i}{S_i} \tag{3}$$

In terms of FSE, both the *average flood storage efficiency* (AFSE) (solid blue line, Figure 5) and the *marginal flood storage efficiency* (MFSE) (dashed red line, Figure 5) can represent a hydrograph shape, yet they focus on different aspects. AFSE describes the peak reduction per unit of flood storage capacity for the whole hydrograph shape, while MFSE focuses on the change of FSE with small additional peak reduction.

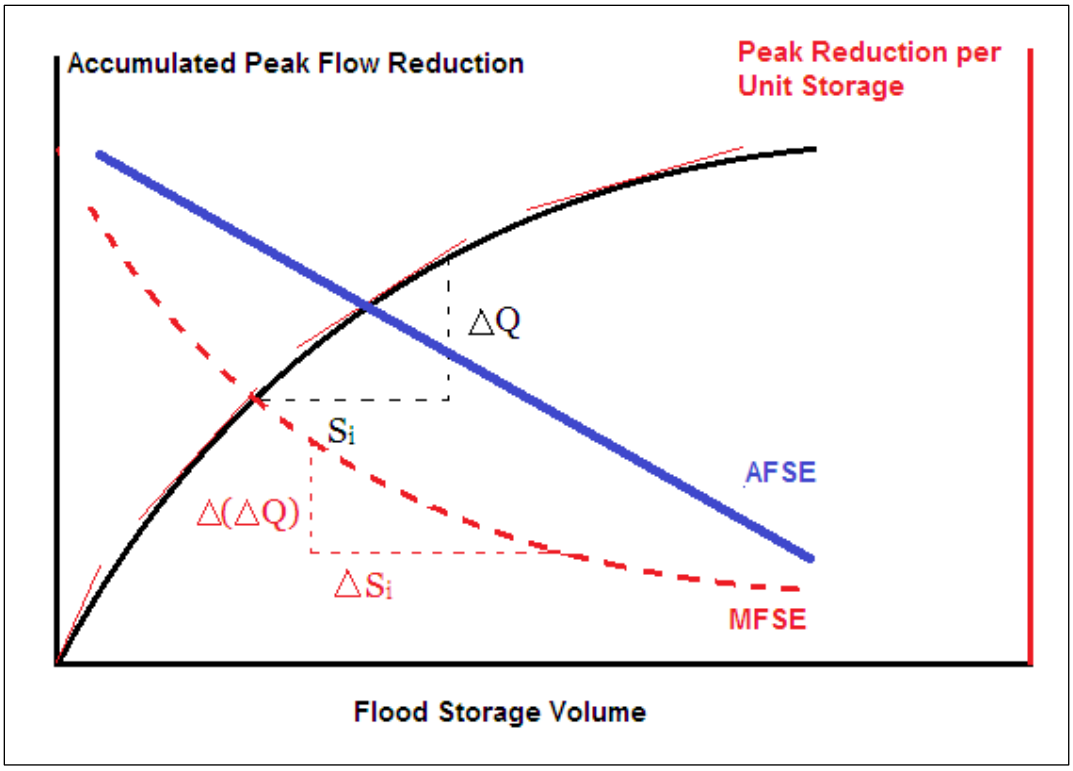

Figure 5. Changes of the relation between peak flow reduction and flood storage volume

The formula of AFSE, with peak inflow $Q_{i,inpeak}$ used instead of maximum peak reduction:

$$AFSE_i = \frac{\overline{\Delta Q_i}}{\overline{S_i}} = \frac{\max\left(\Delta Q_i\right)}{\frac{\alpha_i}{2}\max\left(\Delta Q_i\right)^2 + d_i \max\left(\Delta Q_i\right)} = \frac{1}{\alpha_i Q_{i,inpeak} + 2d_i} \tag{4}$$

The formula of MFSE (the derivative of FSE) is directly calculated from Equation (3),

$$MFSE_i = \frac{\partial \Delta Q_i}{\partial S_i} = \frac{d\Delta Q_i}{dS_i} = \frac{1}{\sqrt{d_i^{\,2} + 2\alpha_i \Delta S_i}} \tag{5}$$

According to Equation (5), MFSE decreases with an increment of flood storage volume ΔS_i . The decreasing MFSE also conforms to the concave function of FSE. Specifically, as flood storage increases, peak flow is reduced, but at a decreasingly effective rate.

3. Deterministic Storage Allocation for a Single Known Storm

3.1 Model and Optimization Formulation

The simple deterministic case consists of two parallel reservoirs and a single known storm (Figure 6). Each reservoir has a particular inflow hydrograph I_{it}, available flood storage capacity S_i, and resulting outflow Q_i. Assuming peak inflows occur at the same time and upstream peak outflows coincide without attenuation or losses (a worst case condition). The downstream peak flow is the summation of peak outflows from two reservoirs: $Q_3 = Q_1 + Q_2$. If ideally operated, each reservoir's outflow will be reduced by utilizing reservoir storage capacity (S_1 and S_2) to store peak flow volumes and minimize downstream flood damage.

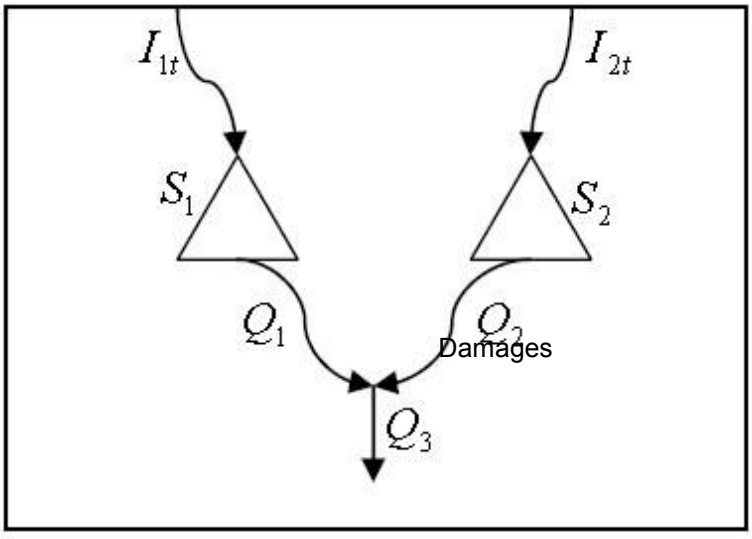

Figure 6. A parallel reservoir system

Given two inflow hydrograph shapes $(i = 1, 2)$ (Figure 7) with base flows B_i, peak inflows $Q_{i,inpeak}$, peak flow durations d_i, rising slopes a_i and recession slopes b_i, the objective is to find optimal flood storage allocations S_i to minimize downstream damage from peak outflows.

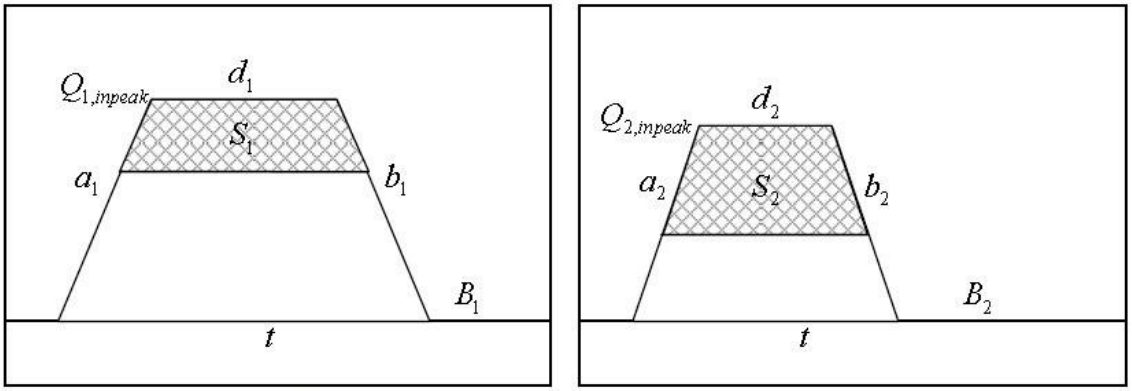

Figure 7. Illustration of flood storage allocation

If downstream damage from peak flow is a non-decreasing function of the combined peak outflows, the objective becomes minimizing the damages of combined peak outflows $D\left(Q_{1,outpeak}+Q_{2,outpeak}\right)$ or $D\left(Q_{1,inpeak}-\Delta Q_1+Q_{2,inpeak}-\Delta Q_2\right)$, where the peak flow reductions correspond to individual allocated flood storages. Storage targets are the real decisions, whereas $\Delta Q_1\left(S_1\right), \Delta Q_2\left(S_2\right)$ are just intermediates.

The optimization problem can be formulated as:

$$Min \qquad z = D\left(Q_{1,outpeak}+Q_{2,outpeak}\right) \tag{6}$$

Subject to:

(1) $S_i \le S_i^{\,0}, \forall i = 1,2$, individual reservoir storage capacity.

(2) $S_1 + S_2 \le S_{Total}$, total flood storage capacity available for allocation.

(3) $Q_{i,outpeak} = Q_{i,inpeak} - \Delta Q_i, \forall i = 1,2$, flow conservation.

(4) $\Delta Q_i = f\left(a_i, b_i, d_i, Q_{i,inpeak}, S_i\right), \forall i$, peak flow reduction.

(5) $Q_i \ge 0, \forall i = 1,2$, non-negative release for each reservoir i.

(6) $\Delta Q_i \ge 0, \forall i = 1,2$, non-negative flow reduction for each reservoir i.

where

$S_i^{\,0}$ = initial reservoir storage capacity

S_{Total} = total flood storage capacity available for allocation.

Other terms are defined as in above.

Damage functions are often approximated with 4 curves. The non-decreasing damage function of flood flow can be linear (curve A), convex (curve B), concave (curve C) or piece wise linear with a threshold (curve D) as illustrated in Figure 8. Curves of

types B and D are more common for flood damage studies. For damage functions with curves A, B and C, the objective of minimizing damage simplifies to peak flow minimization. For damage function like curve D, the objective of minimizing damage becomes minimize the frequency of exceeding the threshold.

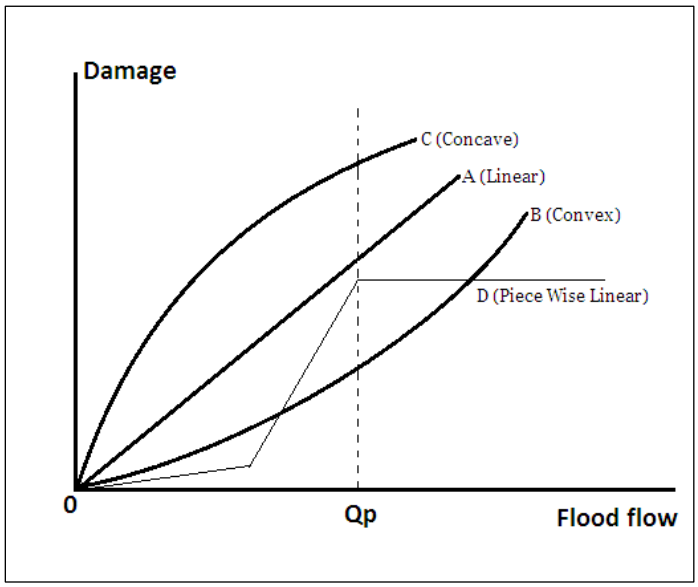

Figure 8. General damage function curves of flood flow

This study assumes the damage functions $D\left(Q_{outpeak}\right)$ are non-decreasing linear (as curve A in Figure 8). Using the generalized form, the optimization formulation for this problem becomes:

$$Min \quad z = \sum_i Q_{i,outpeak}, \forall i = 1,2 \tag{7}$$

Subject to:

$$\Delta Q_i \le \frac{-d_i + \sqrt{d_i^{\,2} + 2\alpha_i S_i^{\,0}}}{\alpha_i}, \alpha_i = \frac{a_i + b_i}{a_i b_i} \tag{8}$$

$$S_1 + S_2 \le S_{Total} \tag{9}$$

$$Q_{i,outpeak} = Q_{i,inpeak} - \Delta Q_i \tag{10}$$

$$\sum_i \Delta Q_i \le \sum_i Q_{i,inpeak} - Q^T \tag{11}$$

$$\Delta Q_i \le Q_{i,inpeak} \tag{12}$$

$$\Delta Q_i \ge 0 \tag{13}$$

3.2 Solutions

Where storage capacity constraints are not binding, the optimal storage allocation can be derived analytically. Ideally, one would allocate storage to provide the same marginal improvement in peak flow reduction (same as the MFSE defined above) for each reservoir in parallel. So a small shift of flood volume or storage capacity from S_i to S_j cannot improve the overall performance of the system. This condition sets the flood storage volumes for reservoirs *i* and *j* so that:

$$\frac{d\Delta Q_i}{dS_i} = \frac{d\Delta Q_j}{dS_j}, \forall i, j \text{ , for each flood, or } \frac{\partial \Delta Q_i}{\partial S_i} = \frac{\partial \Delta Q_j}{\partial S_j}. \quad (14)$$

Then for our generalized trapezoidal hydrograph shape, we can derive the following relation:

$$\frac{1}{\sqrt{d_i^{\,2} + 2\alpha_i S_i}} = \frac{1}{\sqrt{d_j^{\,2} + 2\alpha_j S_j}} \text{ , or } d_i^{\,2} + 2\alpha_i S_i = d_j^{\,2} + 2\alpha_j S_j . \quad (15)$$

$$\text{Along with: } \sum_{i-1}^{n} S_i = S_{Total} . \quad (16)$$

When flood storage volumes allocated to each reservoir can satisfy both Equation (15) and Equation (16), they will have optimal allocations.

To illustrate how MFSEs of two reservoirs affect optimal allocations, the changes of each parallel reservoir's MFSE with changes of storage allocations are in Figure 9.

In Figure 9, for a given fixed total flood storage capacity available for allocation, as flood storage in reservoir 1 increases, flood storage in reservoir 2 decreases correspondingly. Accordingly, the MFSE of reservoir 1 decreases as flood storage volume in reservoir 1 increases, and the MFSE of reservoir 2 increases as flood storage volume in reservoir 2 decreases. At a specific storage allocation proportion, the MFSE of reservoir 1 equals to the MFSE of reservoir 2. Since flood storage volumes of two reservoirs satisfy Equation (16) and the MFSEs satisfy Equation (15), this specific storage allocation is the optimal allocation.

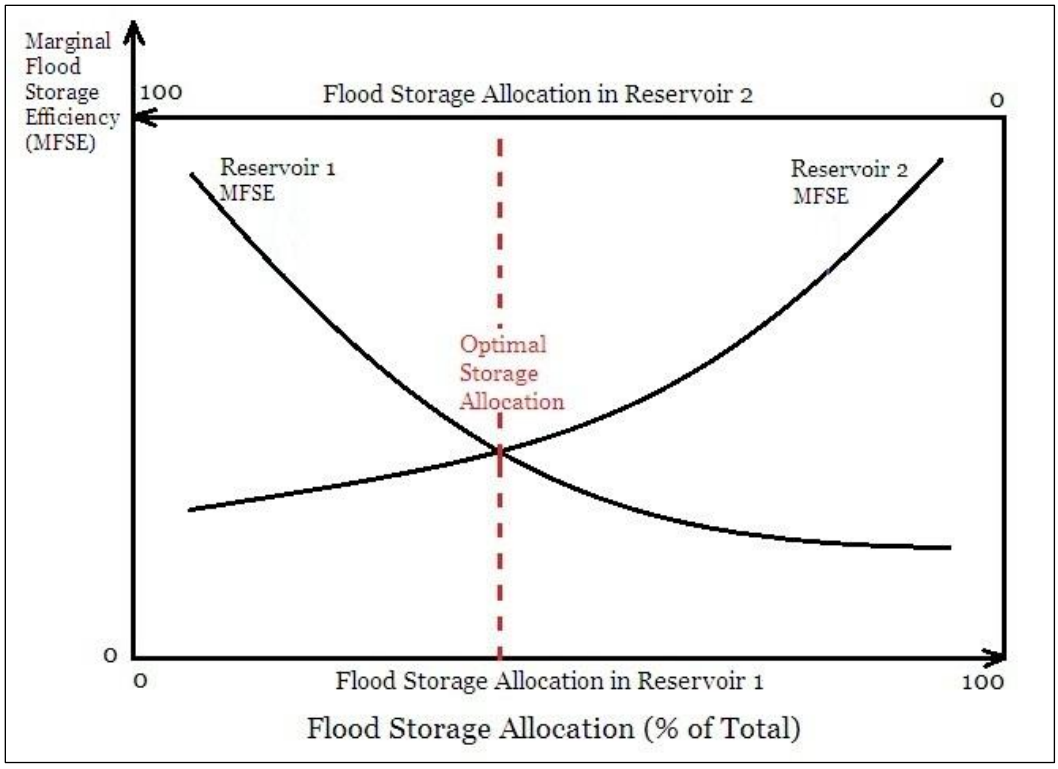

Figure 9. MFSE changes with storage allocation changes between two parallel reservoirs

3.3 Effects of Constraints

This simple deterministic model has six types of constraints: individual storage capacity, peak flow reduction, non-negative outflow, non-negative peak flow reduction, total flood storage capacity and flow conservation. These constraints can be categorized into two groups. One group of constraints can only affect one reservoir at a time, such as reservoir capacity constraints. The other group can affect two reservoirs simultaneously, such as the flow conservation constraint. Below, the effects of individual reservoir capacity and non-negative flow constraints from the first group, and total peak flow reduction constraint from the second group are examined.

3.3.1 Individual Reservoir Capacity

Figure 10 shows the allocation of total flood storage capacity as larger inflow events occur. The two reservoirs in this example have the same individual storage capacities and they regulate inflow storms the same volume with different shapes. The hydrograph entering reservoir 1 is more peaked, while the hydrograph entering reservoir 2 is broader in nature. Because of the different inflow hydrograph shapes, percentages of total flood storage capacity shared by each reservoir differ. Before either storage capacity constraint binds, percent allocations of total flood storage capacity of each reservoir are constant with the same decreasing balanced MFSEs. As total flood storage capacity increases, MFSEs decrease as broader parts of the peak inflows are stored. Then when total flood storage capacity increases to 175 (the first vertical line in Figure 10), reservoir 1 has no more physical capacity to store water (reservoir 1 fills first here). After reservoir 1 fills, all further increased total flood storage capacity is allocated to reservoir 2, which

decreases the MFSE of reservoir 2 (at a faster rate) while the MFSE of reservoir 1 remains unchanged. The percent allocations then converge when reservoir 2 also becomes full (here when the total flood storage capacity exceeds 200-the second vertical line in Figure 10). After convergence, the percent allocations are constant again since no more flood volume can be stored in either fully used reservoir. The two MFSEs also become constant.

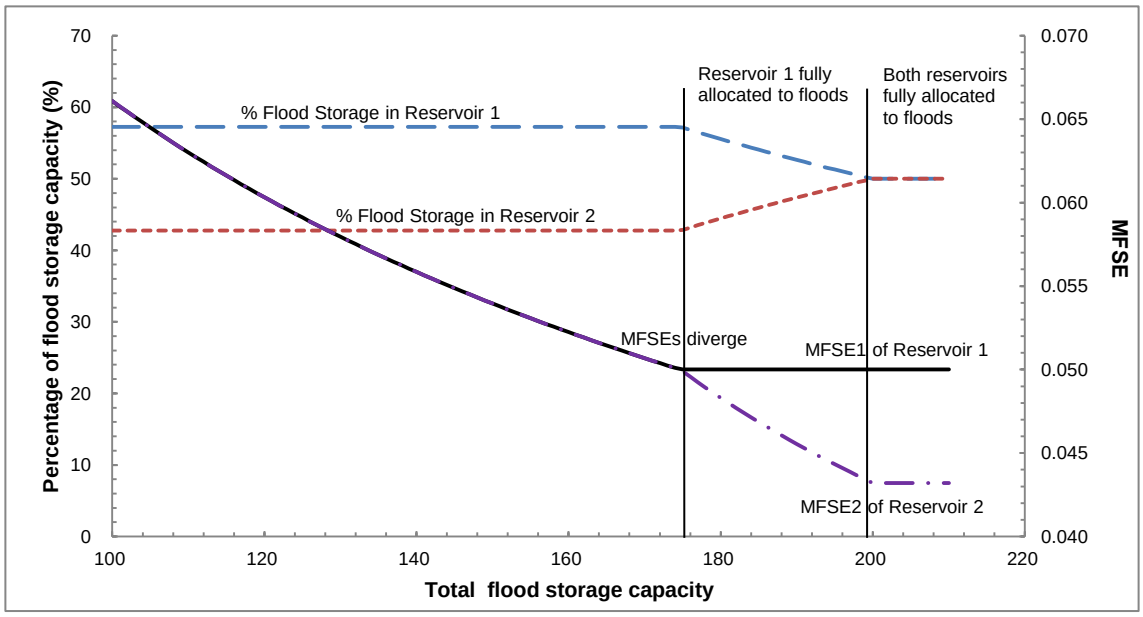

Figure 10. Changes of optimal flood storage allocation and MFSEs of each parallel reservoir with changes of total flood storage capacity affected by the individual reservoir capacity constraint

3.3.2 Non-negative Release

A reservoir cannot store more water than is supplied by inflow. Essentially, releases cannot be negative. This can limit peak flow reduction, even when storage capacity is available. In this example (Figure 11), two reservoirs have the same storage capacities. With less inflow, reservoir 2 is allocated a smaller percentage of total flood storage initially. When total flood storage capacity exceeds 314 (the vertical line in Figure 11), the non-negative release constraint begins to bind on reservoir 2. So reservoir 2 cannot further reduce its peak inflow. Additional total flood storage beyond 314 is entirely allocated to reservoir 1, leading to the gradual divergence of percent allocations. In addition, the trends of MFSEs in Figure 11 are similar to those in Figure 10.

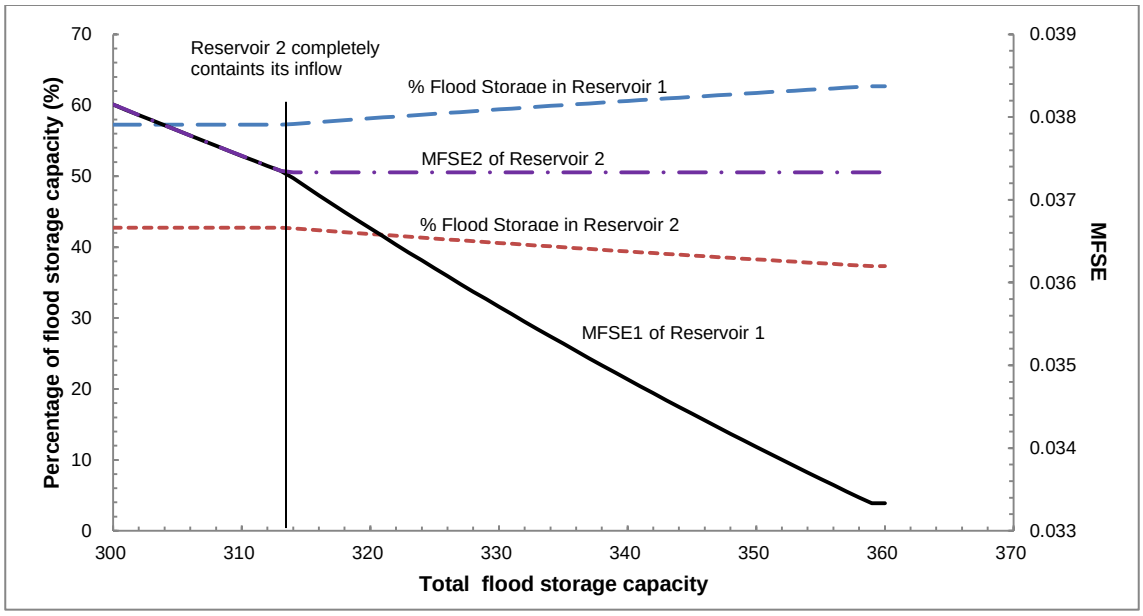

Figure 11. Changes of optimal flood storage allocation and MFSEs of each parallel reservoir with changes of total flood storage capacity affected by the non-negative release constraint

3.3.3 Peak Flow Reduction

The summed peak flow reductions will reach the desired downstream flow target when total flood storage capacity is large enough (Figure 12). In addition, because this constraint binds on the total peak flow reduction, outflows from both reservoirs will be affected simultaneously. So when the downstream outflow reaches the downstream flow target, both reservoirs stop storing flood water. Then percent allocations and MFSEs all become constant. From Figure 12, there are no changes in percent allocations of each reservoir before or after the peak flow reduction constraint binds. However, the effect of this constraint can be seen by the changes of the two identical MFSEs. Clearly, once the downstream target is met (at total flood storage capacity of 129--the vertical line in Figure 12), MFSEs become constant instead of decreasing.

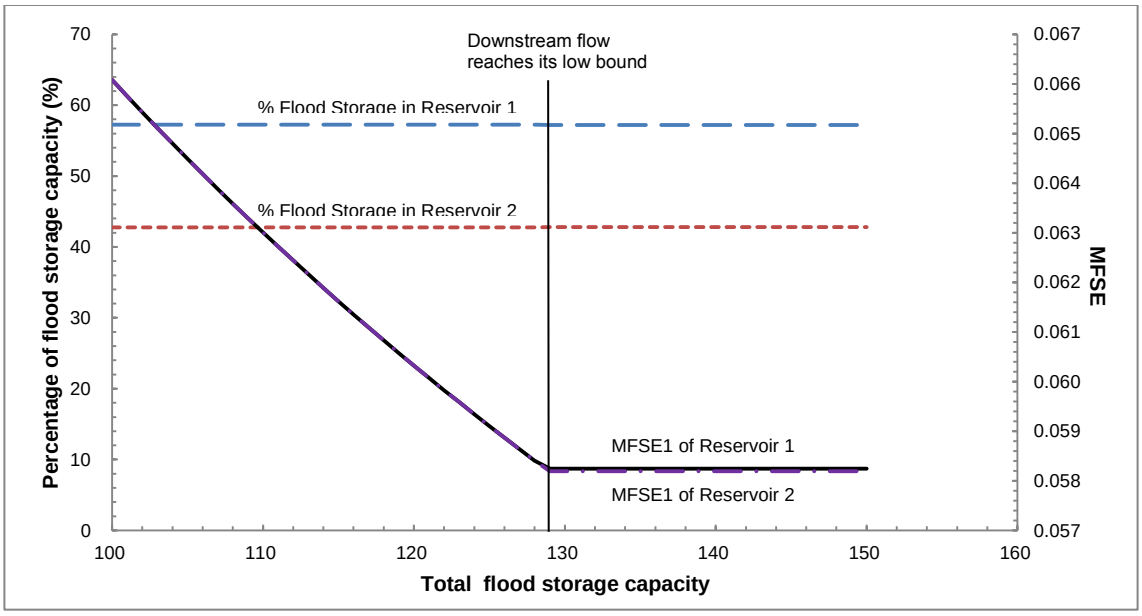

Figure 12. Changes of optimal flood storage allocation and MFSEs of each parallel reservoir with changes of total flood storage capacity affected by the peak flow reduction (downstream release target) constraint

In all these constraint effect analyses, the MFSE of reservoir 1 equals to the MFSE of reservoir 2 if ideally operated. However, if any constraint binds, ΔQ_1 or ΔQ_2 would be restricted within feasible solutions, and equal MFSEs (Equation (14)) cannot be achieved. Numerical optimization is needed for these cases.

As seen in Figures 10, 11 and 12, before any constraints bind, the two MFSEs are ideally identical, as seen by the constant percentages of total flood storage allocated for each reservoir. Meanwhile, MFSEs decrease with increasing total flood storage capacity for both reservoirs, due to diminishing marginal benefits of additional flood storage capacity. However, if any constraint begins to bind, the two MFSEs diverge.

3.4 Hydrograph Effects

Since MFSE is derived from the relationship of peak flow reduction and flood storage volume, hydrograph shape will directly affect a reservoir's MFSE. This in turn will affect the optimal storage allocation in a parallel reservoir system.

3.4.1 Theory

Theoretically, a reservoir with higher MFSE should be allocated more total flood storage capacity because it can accomplish more peak flow reduction per unit of allocated flood storage capacity. However, the MFSE of a reservoir varies with the expected hydrograph shape.

To compare the influence of two reservoirs' hydrograph shapes for various conditions, we introduce a relative form of MFSE—*Relative Hydrograph Shape* (RHS). RHS is defined as the ratio of two MFSEs given a specific flood storage allocation ΔS_i and ΔS_j, as Equation (17) shows:

$$RHS_{ij} = \frac{MFSE_i}{MFSE_j} = \frac{\frac{1}{\sqrt{d_i^{\,2} + 2\alpha_i \Delta S_i}}}{\frac{1}{\sqrt{d_j^{\,2} + 2\alpha_j \Delta S_j}}} = \frac{\sqrt{d_j^{\,2} + 2\alpha_j \Delta S_j}}{\sqrt{d_i^{\,2} + 2\alpha_i \Delta S_i}} \tag{17}$$

Thus at unconstrained optimum:

$$\begin{aligned} &MFSE_i = MFSE_j \\ &RHS_{ij} = 1 \\ &d_i^{\,2} + 2\alpha_i \Delta S_i = d_j^{\,2} + 2\alpha_j \Delta S_j \\ &\Delta S_j = \left\lceil \frac{\left(d_i^{\,2} - d_j^{\,2}\right)}{2\alpha_j} + \frac{\alpha_i}{\alpha_j} \Delta S_i \right\rceil \end{aligned} \tag{18}$$

In addition, we use RHS_{50} referring to the RHS at an equal 50% flood storage allocation to each reservoir, in other words, when total flood storage is equally allocated to two reservoirs, as Equation (18) shows:

$$RHS_{50,ij} = \frac{\sqrt{d_j^{\,2} + 2\alpha_j \bullet \frac{1}{2} S_{Total}}}{\sqrt{d_i^{\,2} + 2\alpha_i \bullet \frac{1}{2} S_{Total}}} = \frac{\sqrt{d_j^{\,2} + \alpha_j S_{Total}}}{\sqrt{d_i^{\,2} + \alpha_i S_{Total}}} \tag{19}$$

When RHS is one, two reservoirs have equal MFSEs. Particularly, if two reservoirs have the identical inflow hydrograph shapes, they would be ideally allocated 50% of total flood storage capacity and RHS_{50} is one, unless other constraints bind.

When RHS diverges from one, the reservoir with smaller MFSE (e.g. having a broader inflow hydrograph shape) should decrease its flood storage allocation while the other reservoir should increase its flood storage, until finally both reservoirs have the same MFSEs. Here, because only the hydrograph shape for reservoir 2 is changing in all hydrograph shape combinations (see Figure 13), MFSE corresponding to 50% of the total flood storage capacity varies for reservoir 2 but is always fixed for reservoir 1. Formed as a relative ratio of hydrograph shapes, the optimal allocation of $RHS_{ij} = MFSE_i / MFSE_j$ should be symmetrical to the optimal allocation of $RHS_{ji} = MFSE_j / MFSE_i$ for any *i* and *j*. For example, the results of combination (2) and (4) are symmetrical, and the results of combination (1), (3) and (9) are themselves symmetrical. In summary, for two parallel reservoirs, the effect of flood hydrograph shape on flood storage allocation as represented by RHS_{50} is as follows:

$$RHS_{50,ij} = \frac{MFSE_{50,i}}{MFSE_{50,j}} \begin{cases} > 1 \text{ more flood storage is allocated to reservoir i} \\ = 1 \text{ flood storage is ideally allocated at a 50\% each} \\ < 1 \text{ more flood storage is allocated to reservoir j} \end{cases} \tag{20}$$

For ideal optimal allocation, MFSEs should be equalized between two parallel reservoirs, unless prohibited by constraints.

3.4.2 Changing Hydrograph Shapes with the Same Inflow Volumes

Here, the two reservoir inflows are given the same flood volumes and one of the hydrograph shapes is varied. As the rising or recession limbs become steeper, or the flood duration becomes shorter, peak inflow will increase for a fixed flood volume. With different hydrograph shape combinations assigned to reservoir 1 and reservoir 2, we analyze the influence of hydrograph shape on flood storage allocation. Nine hydrograph shape combinations are analyzed and summarized in Figure 13. In all the following discussions, RHS_{50} refers to the $RHS_{1,2} = MFSE_1 / MFSE_2$ at a 50% split in total flood storage.

Each number in Figure 13 represents one combination of hydrograph shapes. Inflow volumes and total flood storage capacity are constant, so flood storage allocations to two reservoirs are fixed for calculation of RHS_{50} at an equal 50% total flood storage allocation, whereas RHS_{50} itself changes with the changes of hydrograph shapes. Hydrograph shape for reservoir 1 is always fixed, while hydrograph shape for reservoir 2 widens from steeper to flatter. As a result, the MFSE of reservoir 2 corresponding to 50% of the total flood storage capacity is decreasing and RHS_{50} increases accordingly. For instance, in case (1), the hydrograph shape of reservoir 1 remains triangular (a frontal storm with $a_1 = b_1 = 1$). The hydrograph shape for reservoir 2 is also triangular, but is widening from an abrupt storm shape to a broader snow melt shape. As rising and recession limb slopes of reservoir 2 inflows equally decrease ($a_2 = b_2 = 3, 2.9, ..., 0.5$), MFSE of reservoir 2 for the 50% of total flood storage capacity decreases and RHS_{50} increases. As another example, in hydrograph shapes combination (2), the hydrograph shape for reservoir 1 remains unchanged as a frontal storm ($a_1 = b_1 = 1$). The hydrograph shape of reservoir 2 is an abrupt wave. As the recession limb of reservoir 2 widens from steeper to flatter ($a_2 = +\infty, b_2 = 3, 2.9, ..., 0.2$), MFSE of reservoir 2 for the 50% of total flood storage capacity decreases and RHS_{50} increases.

3.4.2.1 Constant Flood Volume and Constant Total Flood Storage Capacity

For nine combinations of two parallel reservoirs' hydrograph shapes, the optimal percentage changes due to changes of RHS_{50} are shown in Figure 13. Both flood volume (300 here) and total flood storage capacity (200 here) are fixed for each condition.

As MFSE of reservoir 2 calculated for a 50% total flood storage allocation and RHS_{50} (also calculated for a 50% storage allocation) increase, percent allocation of reservoir 1 (the blue stars) increases, while that of reservoir 2 (the red dots) decreases correspondingly. Flood storage volume is optimally allocated to reservoirs with higher MFSE to eventually equalize the MFSEs of two reservoirs. In addition, when both hydrograph shapes are flood pulses as in condition (9), optimal allocations reverse abruptly within a small region. This special case is due to the characterization of a flood pulse hydrograph shape that MFSE is only determined by peak inflow duration. Total flood storage capacity is entirely allocated to the reservoir with shorter peak inflow duration and bigger MFSE under condition (9), unless other constraints intervene.

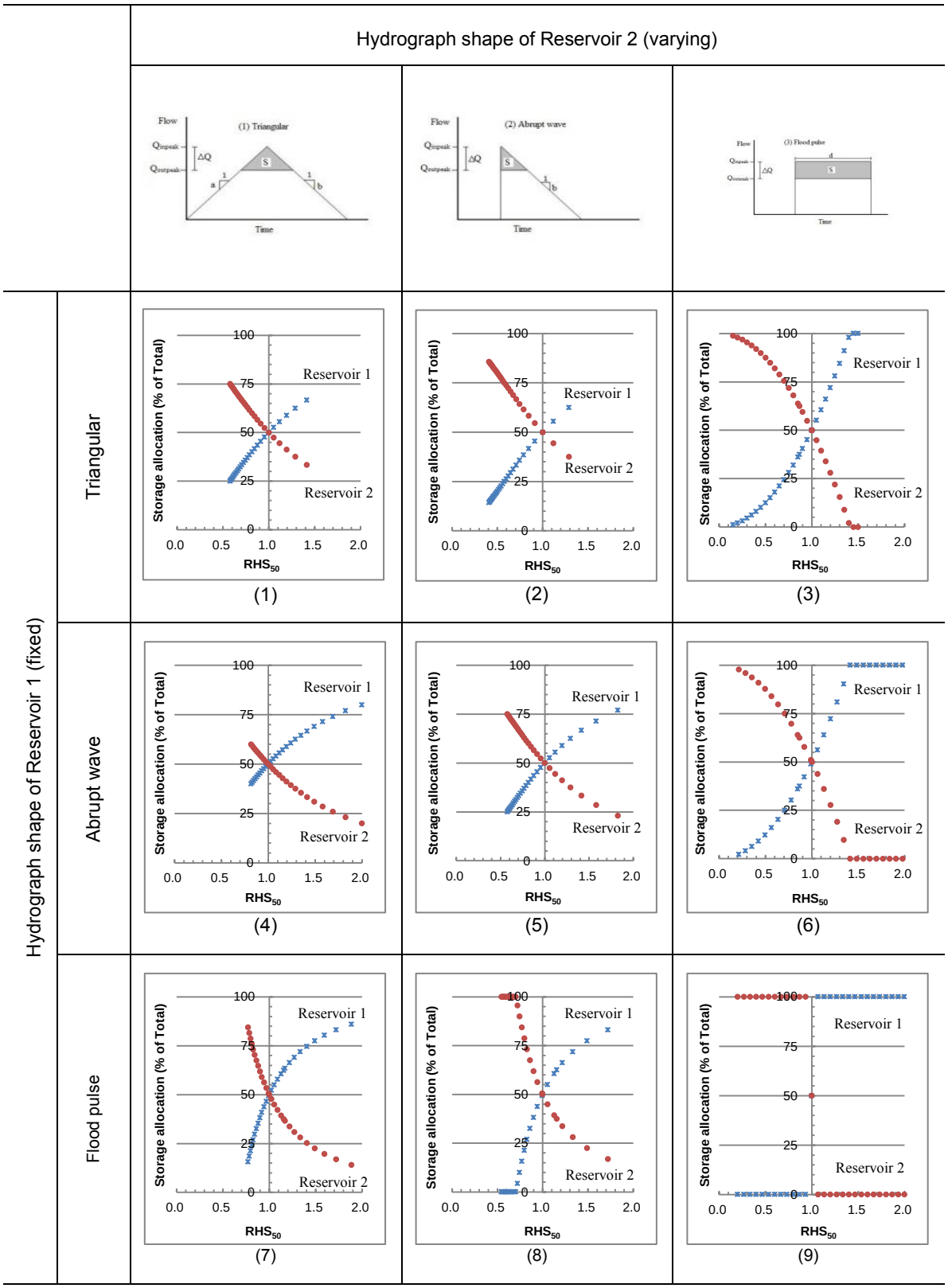

Figure 13. Changes of optimal flood storage allocations with changes of RHS_{50} for two parallel reservoirs for nine combinations of hydrograph shapes storage. Blue stars and red dots are the percent allocations of reservoir 1 and reservoir 2 respectively.

Though reservoir 1 itself has no changes under each condition, MFSE of reservoir 2 becomes smaller and RHS_{50} grows as the hydrograph shape of reservoir 2 widens. The changes of reservoir 2 inflows lead to more flood volume stored in reservoir 1 and MFSEs of both reservoirs decreasing. Ideally, two MFSEs would be identical. Figure 14 shows optimal MFSEs for each combination of hydrograph shapes, the solid blue line is MFSE of reservoir 1 with an unchanged hydrograph shape while the dash red line is MFSE of reservoir 2 with a widening hydrograph shape (varying from steeper to flatter with fixed flood volume). For most combinations, MFSEs of the two reservoirs equally change with changes of RHS_{50} (calculated for an equal 50% storage allocation). Only for hydrograph shape combinations (6), (8) and (9), the two reservoirs' MFSEs differ due to non-negative peak flow reduction constraints. Besides, MFSEs of unchanged flood pulse hydrograph shapes are always constant, since MFSE will not change with allocated flood storage volume for a fixed rectangular hydrograph.

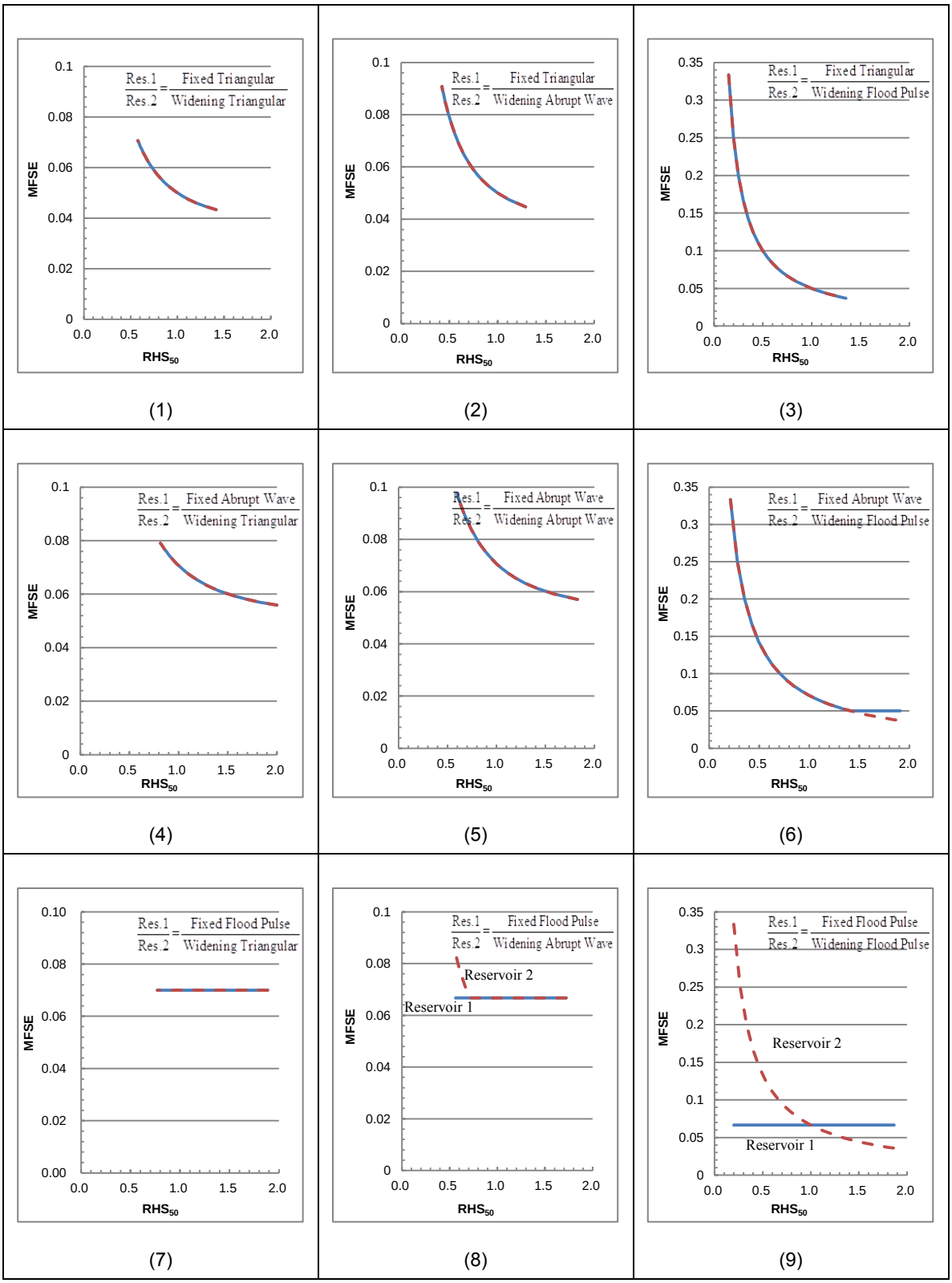

Figure 14. Changes of optimal MFSEs with changes of RHS_{50} for nine combinations of hydrograph shapes for two parallel reservoirs. Blue solid lines are the MFSEs of reservoir 1. Red dash lines are the MFSEs of reservoir 2.

To better illustrate the similarities and differences of the MFSEs changes with the changes of relative hydrograph shape, curves of comparable hydrograph shape combinations are plotted on the same graph (Figure 15). Figure 15 (a) includes curves in hydrograph shape combinations (1), (2), and (3) where the hydrograph shapes of reservoir 1 are fixed triangular and the hydrograph shapes of reservoir 2 are widening triangular, abrupt wave and flood pulse; Figure 15 (b) includes curves in hydrograph shape combinations (1), (4), and (7) where the hydrograph shapes of reservoir 1 are fixed triangular, abrupt wave and flood pulse and the hydrograph shapes of reservoir 2 are widening triangular; Figure 15 (c) includes curves in hydrograph shape combinations (4), (5), and (6) where the hydrograph shapes of reservoir 1 are fixed abrupt wave and the hydrograph shapes of reservoir 2 are widening triangular, abrupt wave and flood pulse; Figure 15 (d) includes curves in hydrograph shape combinations (2), (5), and (8) where the hydrograph shapes of reservoir 1 are fixed triangular, abrupt wave and flood pulse and the hydrograph shapes of reservoir 2 are widening abrupt wave; Figure 15 (e) includes curves in hydrograph shape combinations (7), (8), and (9) where hydrograph shapes of reservoir 1 are fixed flood pulse and the hydrograph shapes of reservoir 2 are widening triangular, abrupt wave and flood pulse; Figure 15 (f) includes curves in hydrograph shape combinations (3), (6), and (9) where the hydrograph shapes of reservoir 1 are fixed triangular, abrupt wave and flood pulse and the hydrograph shapes of reservoir 2 are widening flood pulse. Since the MFSEs of two reservoirs change in the same way in hydrograph shape combinations (1), (2), (3), (4) and (7), only one MFSE curve is plotted for these conditions. So each figure in Figure 15 includes three to five curves of MFSEs changes with increasing RHS_{50}.

Compared to the big effects on optimal allocation from changes of flood pulse hydrograph shape in Figure 15, a small change of a triangular or abrupt wave hydrograph shape only slightly affects the optimal allocation of flood storage capacity. So for forecasted triangular or abrupt wave hydrograph shapes, a small forecasting error will only shift the optimal allocation a little. However, optimal operation for a pulse hydrograph shape becomes difficult; even a small forecasting error can greatly change the optimal allocation.

The curves in each graph of Figure 15 have similar patterns of MFSEs, except for hydrograph combinations contain flood pulses. Comparing the three graphs on the left side, Figure 15 (a), (c) and (e). For any fixed hydrograph shape of reservoir 1, the MFSE curves overlap or have similar patterns when the widening hydrograph shape of reservoir 2 is triangular or abrupt wave. Whereas the MFSE curves differ when widening hydrograph shape of reservoir 2 is a flood pulse. Comparing the three graphs on the right side, Figure 15 (b), (d) and (f), results are similar to the left side. For a widening hydrograph shape of reservoir 2, the MFSE curves overlap or have similar patterns when fixed hydrograph shape of reservoir 1 is triangular or abrupt wave. Whereas the MFSE curves differ when fixed hydrograph shape of reservoir 1 is a flood pulse. The reason for these distinguishing optimal allocations with a flood pulse hydrograph shape is the constant MFSE for a given flood pulse hydrograph shape with any flood storage allocation, which is only determined by peak inflow duration. Total flood storage capacity is entirely allocated to the reservoir with shorter peak inflow pulse duration and bigger MFSE, unless other constraints bind.

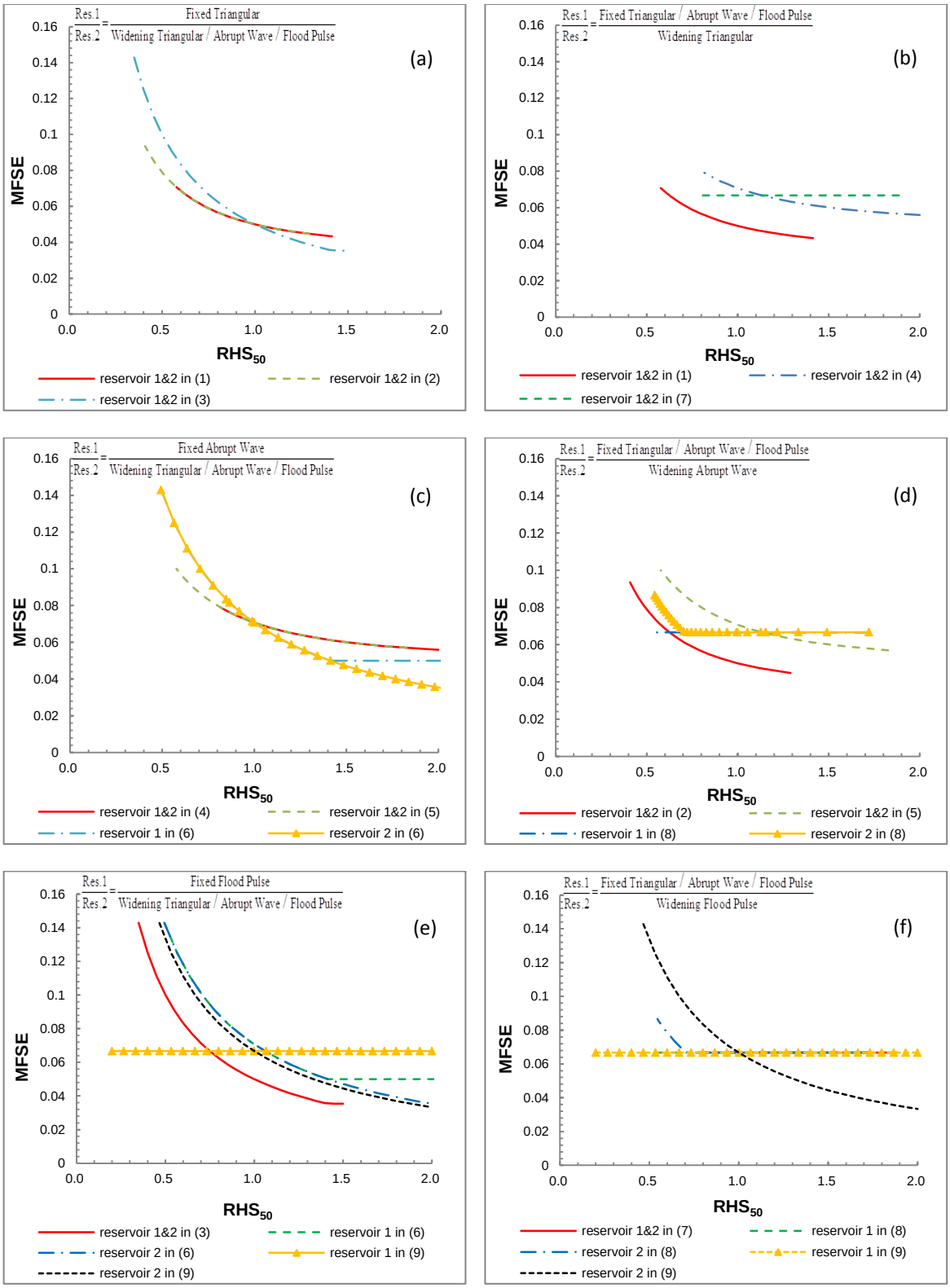

Figure 15. Changes of optimal MFSEs with changes of RHS_{50} calculated for an equal 50% flood storage allocation for two parallel reservoirs. Each figure contains comparable results from Figure 14. 'Res.1' and 'Res.2' refer to hydrograph shape of reservoir 1 and reservoir 2 respectively.

From the above observations, we can conclude that ideal allocation of total flood storage is to equalize the MFSEs of two reservoirs when possible. The ideal allocation or optimal MFSEs of two parallel reservoirs are determined by relative hydrograph shape at an equal 50% total flood storage allocation (RHS_{50}). For different hydrograph shape combinations that reservoir 1 is fixed triangular or abrupt wave or flood pulse and reservoir 2 is varying triangular or abrupt wave or flood pulse, ideal allocation or optimal MFSEs of two parallel reservoirs are following a similar pattern, except for when one of the hydrograph shapes is a flood pulse.

3.4.2.2 Constant Flood Volume and Changing Total Flood Storage Capacity

To further examine hydrograph shape combinations, we can change either the total flood storage capacity available for allocation or the incoming flood volume, leaving the other unchanged. Following are two examples: 1) reservoir 1 has a fixed triangular hydrograph shape and reservoir 2 has a widening triangular hydrograph shape (hydrograph shape combination (1)); 2) reservoir 1 has a fixed triangular hydrograph shape and reservoir 2 has a widening abrupt wave hydrograph shape (hydrograph shape combination (2)).

Here, flood volume for each reservoir is fixed at 300 and total flood storage capacity is changing. Figure 16 shows how optimal allocation changes with changes of RHS_{50} (calculated for an equal 50% storage allocation) for constant flood volume and changing total flood storage capacity.

The left graph in Figure 16 is when the hydrograph shape of reservoir 1 is fixed triangular and hydrograph shape of reservoir 2 is widening triangular (hydrograph shape combination (1)). The percent allocations of each reservoir do not depend on total flood storage capacity, but only change with relative hydrograph shape RHS_{50} calculated for an equal 50% storage allocation. Percent allocations differ only when peak flow reduction constraint (Equation (9)) is binding, specifically when total flood storage exceeds 300 and RHS_{50} exceeds 1.

The right graph in Figure 16 is when hydrograph shape of reservoir 1 is fixed triangular and hydrograph shape of reservoir 2 is widening abrupt wave (hydrograph shape combination (2)). As RHS_{50} increases from 0.4 to 1, the optimal allocations are identical with different total flood storage capacities. Same conclusions can be drawn as in the left graph. Ideally, percent allocations do not depend on total flood storage capacity for a fixed flood volume, but only change with the relative hydrograph shape at an equal 50% storage allocation represented by RHS_{50}.

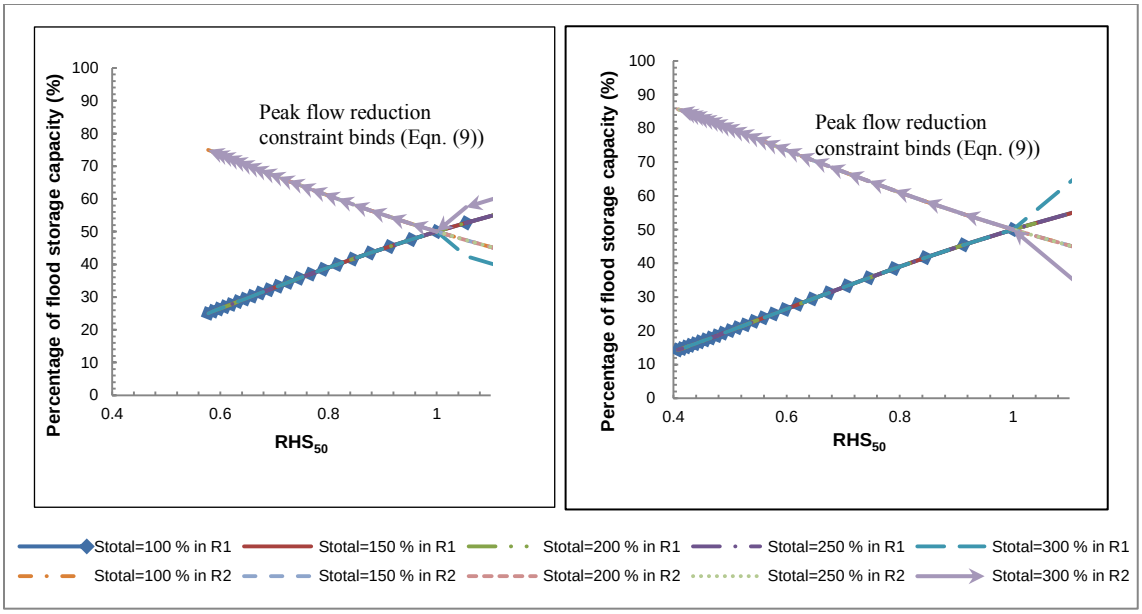

Figure 16. Changes of optimal allocations with increasing RHS_{50} for constant flood volume and changing total flood storage capacity. Left graph: hydrograph shapes combination (1) (both triangular). Right graph: hydrograph shapes combination (2) (abrupt wave and triangular)

3.4.2.3 Changing Flood Volume and Constant Total Flood Storage Capacity

Here, total flood storage capacity is fixed at 200 and the incoming flood volume for each reservoir is varying. Figure 17 shows the changes of percent allocations due to changes of RHS_{50} for constant total flood storage capacity and changing flood volume.

The left graph in Figure 17 is when the hydrograph shape of reservoir 1 is fixed triangular and hydrograph shape of reservoir 2 is widening triangular (hydrograph shape combination (1)). The percent allocations of each reservoir do not depend on flood volume, but only change with relative hydrograph shape RHS_{50} calculated for an equal 50% storage allocation. Only for when peak flow reduction constraint (Equation (9)) is binding, specifically when flood volume is 250 and RHS_{50} exceeds 1.3, percent allocations differ.

The right graph in Figure 17 is when hydrograph shape of reservoir 1 is fixed triangular and hydrograph shape of reservoir 2 is widening abrupt wave (hydrograph shape combination (2)). As RHS_{50} increases from 0.4 to 1, the optimal allocations for all different flood volume conditions are the same. Same conclusions can be drawn as in the left graph. Ideally, percent allocations of total flood storage capacity do not depend on the flood volume for a fixed total flood storage capacity, but only change with the relative hydrograph shape at an equal 50% storage allocation represented by RHS_{50}.

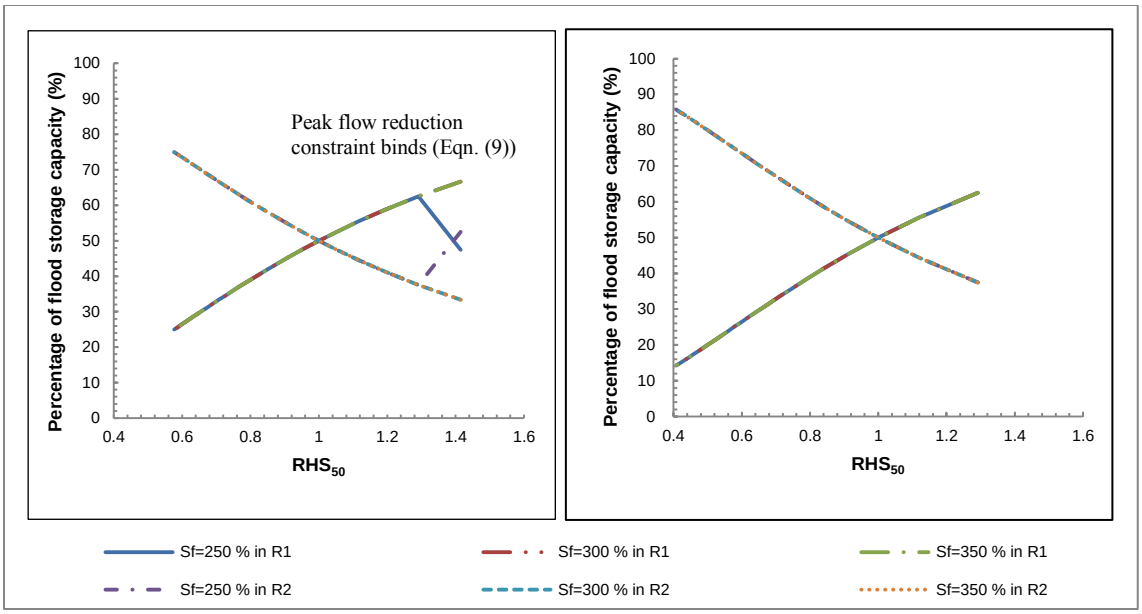

Figure 17. Changes of optimal allocations with increasing RHS_{50} for changing flood volume and constant total flood storage capacity. Left graph: hydrograph shapes combination (1) (both triangular). Right graph: hydrograph shapes combination (2) (abrupt wave and triangular)

From the discussions in the above section 3.4.2.2 and 3.4.2.3, ideal flood storage allocation among two parallel reservoirs can be simply determined by the relative hydrograph shape RHS_{50} at an equal 50% storage allocation, for whether constant flood volume and changing total flood storage capacity condition, or constant total flood storage capacity and changing flood volume condition, unless constraints bind. In other words, relative hydrograph shape RHS_{50} at an equal 50% storage allocation dominates the optimal flood storage allocation among parallel reservoir, while total flood storage capacity and flood volume are comparatively less important.

3.4.3 Sensitivity Analysis of Hydrograph Shape

For a given incoming flood volume, the relation of peak flow reduction and flood storage volume varies with hydrograph shape. Here we vary α_i (representing rising limb and recession limb together since they would have the same impacts) and d_i (duration of peak inflow) to examine how sensitive the optimal allocation is to a hydrograph shape *i* ($i = 1, 2$). Additionally, since the flood inflow volumes are fixed for two reservoirs, peak inflow will decrease as either α_i or d_i increases.

The base-case optimal downstream peak flow is 16.01. Four hydrograph parameters are changed from -50% to 50% respectively, including α_1 and d_1 of reservoir 1, and α_2 and d_2 associated with reservoir 2. The optimal results are shown below in Figure 18. Percent change at 0 on the horizontal axis is for the base-case optimization. Changes of total downstream peak flow with varying α_1 and α_2 are plotted based on the left vertical axis, while the comparatively slight changes of total

downstream peak flow with varying d_1 and d_2 are plotted based on the right vertical axis.

In Figure 18, as either α_i (rising and/or recession limb) or d_i (peak inflow duration) increase, the inflow hydrograph shape widens with lower peak inflow and longer duration, and total downstream peak flow decreases. Compared to the changes of d_i, changes of α_i have larger impact on total downstream peak reduction. For a given predicted flood volume, a rapid flood with steeper rising and recession limbs is more dangerous than a mild flood with longer peak duration in terms of reducing downstream peak flow.

Comparing total downstream peak reduction changes due to changes of α_1 (rising and/or recession limb of hydrograph shape of reservoir 1) and α_2 (rising and/or recession limb of hydrograph shape of reservoir 2), α_1 has larger impacts on the optimal results since α_1 is bigger than α_2. Similarly, for the total downstream peak reduction changes due to changes of d_1 (peak inflow duration of hydrograph shape of reservoir 1) and d_2 (peak inflow duration of hydrograph shape of reservoir 2) where d_2 is bigger than d_1, d_2 has larger impacts on the optimal results. Therefore, the curve of changes of α_1 is much steeper than that of α_2, and the curve of changes of d_2 is much steeper than that of d_1. In addition, the impacts of hydrograph shape are irrelevant to reservoirs, but only depend on each individual hydrograph shape parameter.

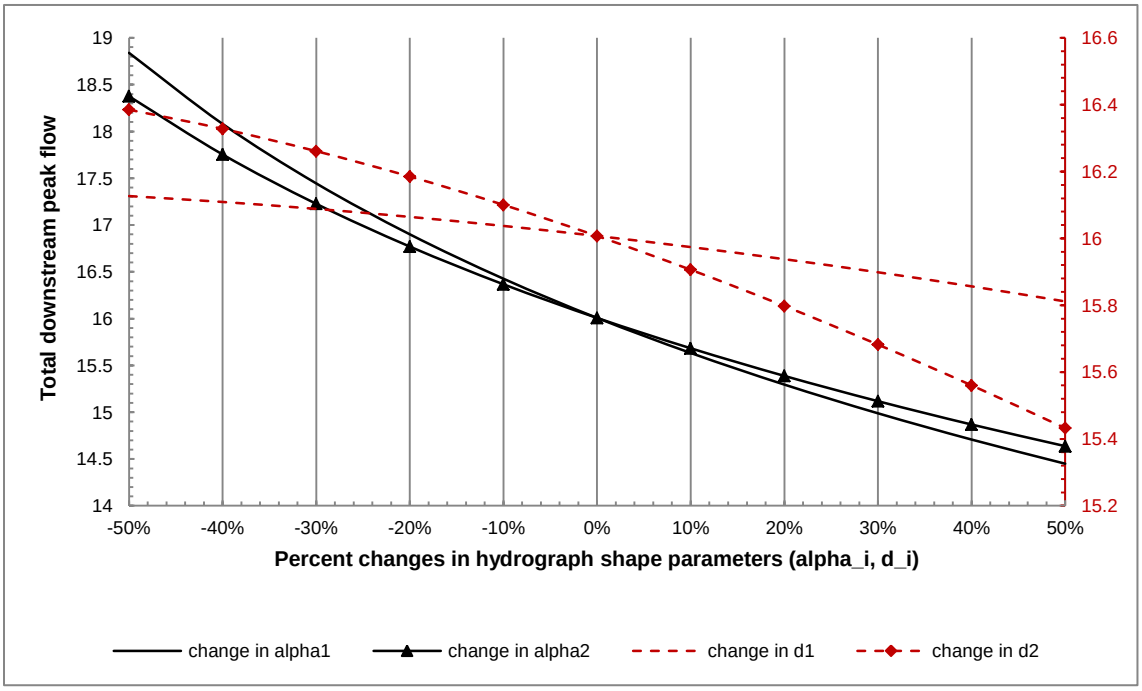

Figure 18. Impacts of hydrograph shape changes on total downstream peak flow (single deterministic storm model)

In conclusion of this sensitivity analysis, optimal allocation is more sensitive to the rising and receding limbs than to the duration of peak inflow. This can be explained that a rapidly occurred flood inflow would leave less time to adjust the reservoir operation than a long lasting peak flow. Worse damage would be most likely caused by a rapidly increasing flood. Additionally, for either rising and recession limbs or peak inflow duration of each reservoir, the impacts are only proportional to their values.

4. An Uncertain Storm for Two Parallel Reservoirs

4.1 General Formulation

Previously, the inflow volumes and hydrograph shapes of each reservoir are assumed to be known. Here the optimal storage allocation considering the uncertainty of future flood hydrograph shapes is explored.

Given a total flood storage availability (S_{Total}), the problem becomes how to allocate flood storage among reservoirs. The following formulation assigns probabilities to a variety of possible incoming hydrographs. The overall objective is to minimize the expected damage caused by the downstream peak flow exceeding the downstream channel capacity.

$$Min \qquad z = \sum_{f=1}^{m} p_f \cdot D\left(\sum_{i=1}^{n} Q_{if,outpeak} \right) \tag{21}$$

Subject to:

$$\Delta Q_i \le \frac{-d_{if} + \sqrt{d_{if}^{\,2} + 2\alpha_{if} S_i^0}}{\alpha_{if}}, \alpha_{if} = \frac{a_{if} + b_{if}}{a_{if} b_{if}}, \forall f = 1, 2 \ldots m \tag{22}$$

$$\sum_{i=1}^{n} S_i \le S_{Total} \tag{23}$$

$$Q_{if,outpeak} = Q_{if,inpeak} - \Delta Q_i, , \forall f = 1, 2 \ldots m, \forall i = 1, 2 \tag{24}$$

$$\sum_{i} \Delta Q_i \le \sum_{i} Q_{if,inpeak} - Q^T, \forall f = 1, 2 \ldots m \tag{25}$$

$$\Delta Q_i \le Q_{if,inpeak}, \forall f = 1, 2 \ldots m \tag{26}$$

$$\Delta Q_i \ge 0 \tag{27}$$

where

p_f = the probability of each flood hydrograph scenario *f*

$Q_{if,inpeak}$ = peak inflow without reduction for an individual reservoir *i* and each hydrograph scenario *f*

$Q_{if,outpeak}$ = peak flow after reduction for an individual reservoir *i* and each hydrograph scenario *f*

$D\left(\sum_{i=1}^{n} Q_{if,outpeak} \right)$ = downstream damage function

$\left(\sum_{i=1}^{n} Q_{if,outpeak} \right)$ = downstream peak flow, which is simplified as the summation of all $Q_{if,outpeak}$ following the assumptions made in the above discussion

ΔQ_i = peak flow reduction for an individual reservoir *i*

S_i^0 = initial storage capacity of reservoir *i*

Q^T = downstream release target (minimum downstream outflow)

S_i = flood storage volume of reservoir *i* associated with ΔQ_i (their relationship can be derived geometrically)

m = number of different hydrograph

n = number of reservoirs.

4.2 Analysis of an Example

We illustrate the analysis with three hydrograph pairs and two reservoirs in parallel, each hydrograph with an equal probability 1/3.

Let the initial storage capacities of reservoir 1 and reservoir 2 be 200 and 180 respectively. Incoming flood volumes are predicted to be 300 for reservoir 1 and 200 for reservoir 2. Downstream release target is 8. Similar to the simple deterministic storage allocation for a single know storm, the damage function here is simplified using a linear form: $D\left(\sum_{i=1}^{n} Q_{if,outpeak} \right) = \sum_{i=1}^{n} Q_{if,outpeak}$. Damage functions in the following discussions are also assumed to be linear with downstream peak. The input data are in Table 1.

Table 1. Inflow data of an uncertain storm with three probable hydrographs

Hydrograph	Expected		H 1		H 2		H 3	
Probability			1/3		1/3		1/3	
Reservoir	R 1	R 2	R 1	R 2	R 1	R 2	R 1	R 2
$\alpha_{if} = \frac{a_{if} + b_{if}}{a_{if} b_{if}}$	1.92	2.08	1.5	2	2.25	2.25	2	2
Duration of peak inflow, d_{if}	0.5	0.33	0	0.5	0.5	0	1	0.5
Peak inflow	17.43*	13.7*	20	13.89	16.11	13.33	16.83	13.89

*Expected peak inflows are derived from predicted inflow volumes and expected parameters of hydrograph shapes, not the expected value of all forecasting peak inflows.

For a total flood storage capacity of 200, the optimal storage allocations from three methods: Deterministic Expected Forecast, Two-stage Forecast and Expected Perfect Forecast are listed below in Table 2.

The first allocation from the Deterministic Expected Forecast method optimizes for the expected hydrograph from three probable hydrographs. The second allocation is from the Two-stage Forecast method (Equations (21) to (27)). Here, allocations minimize the expected value of all individual peak outflows. So this two-stage forecast method can satisfy the peak flow reduction constraints for all hydrographs. The second stage

performance of each uncertain hydrograph given the first stage allocations are also listed in Table 2. The last allocation is from the Expected Perfect Forecast method. This method takes the expected outcomes of three probable hydrographs, which are individually optimized as deterministic hydrographs.

Table 2. Optimal storage allocations for Deterministic Expected Forecast, Two-stage Forecast and Expected Perfect Forecast of three probable hydrograph scenarios for two parallel reservoirs

		Reservoir	Peak flow reduction	Flood storage	MFSE	Optimized downstream peak flow	Actual Expected downstream peak
Deterministic Expected Forecast [(a)]		R1	10.17	104.15	0.05	**11.53**	**11.67**
		R2	9.43	95.85	0.05		
Two-stage Forecast [(b)]		R1	9.21	85.85	0.06	**12.72**	**12.72**
		R2	9.43	95.75	0.05		
Second stage performance of the Two-stage Forecast[(c)]	Hydrograph 1	R1	9.21	63.59	0.07	**15.26**	**15.26**
		R2	9.43	93.62	0.05		
	Hydrograph 2	R1	9.21	99.98	0.05	**10.81**	**10.81**
		R2	9.43	100.02	0.05		
	Hydrograph 3	R1	9.21	93.99	0.05	**12.09**	**12.09**
		R2	9.43	93.62	0.05		
Expected Perfect Forecasts [(d)]		R1	10.35	104.73	0.05	**11.60**	**11.60**
		R2	9.40	95.27	0.05		
Individual Optimization of Expected Perfect Forecast [(e)]	Hydrograph 1	R1	12.35	114.32	0.05	**12.54**	**14.14**
		R2	9.01	85.68	0.05		
	Hydrograph 2	R1	9.21	99.97	0.05	**10.81**	**9.69**
		R2	9.43	100.03	0.05		
	Hydrograph 3	R1	9.51	99.90	0.05	**11.46**	**10.97**
		R2	9.76	100.10	0.05		

(a) Deterministic Expected Forecast method takes the expected value of three probable hydrographs as deterministic input hydrographs.
(b) Two-stage Forecast method minimizes the expected value of all individual outcomes by applying identical decision variables to different hydrographs.
(c) Second stage performance of the Two-stage Forecast.
(d) Expected Perfect Forecast takes the expected value of outcomes from each forecasting hydrograph that is individually optimized as deterministic hydrograph.
(e) Individual deterministic optimization of each hydrograph treated as perfect forecasted.

In terms of minimizing downstream peak flow and equalizing MFSEs, the first Deterministic Expected Forecast method is the best in this example. This method simply uses the expected value of three probable hydrographs as input hydrograph and results in the lowest downstream peak flow (11.53). However, the optimal storage allocation given by the Deterministic Expected Forecast method might not satisfy some of the constraints. For example, when a less probable and significantly small storm occurs, peak flow reduction from the Deterministic Expected Forecast method might exceed peak inflow. So this Deterministic Expected Forecast method is not applicable when the

sizes and probabilities of forecasted uncertain hydrographs differ greatly. Additionally, by applying the optimal peak flow reductions to each individual hydrograph shape, the resulting expected downstream peak flow may differ from the optimized downstream peak flow, as shown in the last two columns for the Deterministic Expected Forecast method. This difference is from the non-linear relation of peak flow reduction and flood storage volume. A more complex shape of damage curve would further change the results.

Downstream peak flow from the Expected Perfect Forecast method is 11.60 in this example, which is very close to the lowest value (11.53). Differing from the Deterministic Expected Forecast method using expected input hydrograph, the Expected Perfect Forecast method takes the expected value of outcomes. When optimizing storage allocation of each individual hydrograph, Expected Perfect Forecast method basically assumes that each hydrograph is perfect forecasted and can be optimized as a deterministic model. For each perfect forecasted hydrograph, MFSEs of two reservoirs should be identical if ideally operated. Similar to the Deterministic Expected Forecast method, constraints violation problem also exists in this Expected Perfect Forecast method. As shown in the last two columns for the Expected Perfect Forecast method, the two expected downstream peak flows are identical. However, when applying optimal peak flow reductions to each individual hydrograph shapes optimized as deterministic models, the resulting expected downstream peak flows differ from the optimized downstream peak flows. Therefore, the Deterministic Expected Forecast and the Expected Perfect Forecast methods are both more suitable with better forecasts.

The Two-stage Forecast method optimizes an expected downstream peak flow of 12.72 for three uncertain hydrographs. This expected value exceeds downstream peak flows from the other two methods. The reason is that the relatively small peak inflow of hydrograph 2 for reservoir 2 binds on the optimal allocation. Besides, MFSEs of uncertain hydrographs are only approximately equal for all three hydrographs and expected value. However, only the Two-stage Forecast method considers all the constraints of each individual uncertain hydrograph. The overall performance and individual performances (second stage performances) are constant for optimized downstream peak flows and actual expected downstream peak flows. So among all these three methods, storage allocation from the Two-stage Forecast method is the most realistic, although it is the worst one in terms of reducing downstream peak flow. In particular, when the size and probable of a coming storm is quite uncertain, the Two-stage Forecast method works the best.

In conclusion, considering the uncertainty in flood forecasting, parallel reservoirs should be operated together to reduce downstream peak flow with appropriate methods. For relatively more certain forecasted storms, the Deterministic Expected Forecast method works most effectively to minimize downstream peak flow and equalize MFSEs. The Expected Perfect Forecast method is also applicable under this condition, although less effective. However, when there are big differences among the sizes and probabilities of forecasted uncertain hydrographs, the Two-stage Forecast method is a better choice. In addition, the (nearly) equal MFSEs again demonstrate the ideal flood operation rules for parallel reservoir: to allocate flood storage equalizing the marginal improvements in peak flow reduction for each reservoir.

5. Series of Storms for Two Parallel Reservoirs

5.1 General Formulation for Known Storms

For a series of perfectly predicted storms coming into two reservoirs in parallel, reservoirs need to store part of or all of the flood volume for each storm. The worst downstream condition will come from the largest downstream peak flow among all the storms due to general non-decreasing damage function of flood flow. Thus the objective becomes to minimize the maximum damage of downstream peak flow among the storms. Moreover, if storms are uncertain, the probability of each storm should also be included in the objective function. The uncertainty of a storm could be reflected in forecasts of incoming flood volume and hydrograph shape.

Given a total flood storage volume $S_{Total} \le \sum_{j=1}^{l} \sum_{i=1}^{n} S_{ij}^{0}$ available for allocation, the problem becomes to optimize individual flood storage volumes S_{ij} ($\sum_{j=1}^{l} \sum_{i=1}^{n} S_{ij} \le S_{Total}$) among the reservoirs.

To find the ideal allocation of total flood storage capacity for a series of storms in a parallel reservoir system, we should minimize the maximum damage of downstream peak inflow.

$$Min \qquad z = \underset{j=1:l}{Max}\, D\left(\sum_{i=1}^{n} Q_{ij,outpeak} \right) \tag{28}$$

Subject to:

$$\Delta Q_{ij} \le \frac{-d_{ij} + \sqrt{{d_{ij}}^2 + 2\alpha_{ij} {S_{ij}}^0}}{\alpha_{ij}}, \alpha_{ij} = \frac{a_{ij} + b_{ij}}{a_{ij} b_{ij}} \tag{29}$$

$$\sum_{j=1}^{l} \sum_{i=1}^{n} S_{ij} \le S_{Total} \tag{30}$$

$${S_{ij}}^0 = {S_{i,j-1}}^0 - S_{ij},\ j = 1, 2, \ldots l \tag{31}$$

$$Q_{ij,outpeak} = Q_{ij,inpeak} - \Delta Q_{ij}, \forall i,\ j \tag{32}$$

$$\sum_{i} \Delta Q_{ij} \le \sum_{i} Q_{ij,inpeak} - Q_j^T \tag{33}$$

$$\Delta Q_{ij} \le Q_{ij,inpeak} \tag{34}$$

$$\Delta Q_{ij} \ge 0 \tag{35}$$

where

$Q_{ij,inpeak}$ = peak inflow without reduction for an individual reservoir *i* and a storm *j*

$Q_{ij,outpeak}$ = peak flow after reduction for an individual reservoir *i* and a storm *j*

$D\left(\sum_{i=1}^{n} Q_{ij,outpeak}\right)$ = downstream damage function

$\left(\sum_{i=1}^{n} Q_{ij,outpeak}\right)$ = downstream peak flow, which is simplified as the summation of all the $Q_{ij,outpeak}$

ΔQ_{ij} = peak flow reduction for an individual reservoir *i* and a storm *j*

S_{ij}^{0} = storage capacity for reservoir *i* before storm *j* happens, the initial reservoir storage capacities of two reservoirs $S_{i,1}^{0} = S_{i}^{0}$ are given

Q_{j}^{T} = downstream release target for a storm *j*

S_{ij} = flood storage volume for reservoir *i* and storm *j* and peak reduction ΔQ_{ij} (their relationship can be derived geometrically)

n = number of reservoirs

l = number of storms.

There are $n \times l$ decision variables in total: $\Delta Q_{ij}\left(i = 1:n;\ j = 1:l\right)$.

5.2 Results and Analysis of Examples

The simple two parallel reservoirs system and three separate storms are used for illustrating the series know storms model.

5.2.1 Input Data and Results

The initial flood storage capacities of reservoir 1 and reservoir 2 are 40 and 25 respectively. Total flood storage capacity available for allocation is set to be the sum of two reservoirs' storage capacities: 65. Minimum release for downstream is set to be 0 for all the three storms. The other input data are listed in Table 3.

Table 3. Inflows data of three certain storms for two parallel reservoirs

	Storm 1		Storm 2		Storm 3	
Reservoir	R1	R2	R1	R2	R1	R2
Inflow volume	20	10	30	20	15	15
$\alpha_{ij} = \frac{a_{ij} + b_{ij}}{a_{ij} b_{ij}}$	1	2	2.25	2.25	2	2
Duration of peak inflow, d_{ij}	0	0.5	0.5	0	1	0.5
Peak inflow	6.32	2.92	4.95	4.22	3.41	3.63

For a total flood storage capacity of 65, the optimal results using non-linear

Generalized Reduced Gradient method are in Table 4.

Table 4. Optimal results of three certain storms in a series for two parallel reservoirs (total flood storage capacity is 65)

	Storm 1		Storm 2		Storm 3	
Reservoir	R1	R2	R1	R2	R1	R2
Flood storage volume	13.18	5.24	17.90	12.48	8.91	7.27
Peak flow reduction	5.14	2.05	3.77	3.33	2.53	2.46
Peak inflow	6.32	2.92	4.95	4.22	3.41	3.63
Outflow	1.19	0.87	1.17	0.89	0.88	1.17
Downstream peak flow	2.06		2.06		2.05	
Maximum Downstream peak flow			2.06			
Total flood storage volume in R1			40			
Total flood storage volume in R2			25			

The optimal results show that reservoir storage capacity constraints are binding on two reservoirs: the two reservoirs both fully use their storage capacity. To reduce the maximum downstream peak flow, one would optimally allocate flood storage capacity to equalize downstream peak flow of each storm under the constrained condition. For instance in Table 4, downstream peak flows for Storm 1, 2 and 3 are 2.06, 2.06 and 2.05 respectively.

If total flood storage capacity available for allocation is reduced to be 55, the optimal results are shown in Table 5.

Table 5. Optimal results of three certain storms in a series for two parallel reservoirs (total flood storage capacity is 55)

	Storm 1		Storm 2		Storm 3	
Reservoir	R1	R2	R1	R2	R1	R2
Flood storage volume	10.49	5.36	12.95	12.99	6.56	6.65
Peak flow reduction	4.58	2.08	3.18	3.40	2.11	2.34
Peak inflow	6.32	2.92	4.95	4.22	3.41	3.63
Outflow	1.74	0.84	1.77	0.82	1.29	1.29
Downstream peak flow	2.59		2.59		2.59	
Maximum Downstream peak flow			2.59			
Total flood storage volume in R1			30			
Total flood storage volume in R2			25			

In this case, total flood storage volume of reservoir 1 is 30 and its capacity is not fully used, while total flood storage volume of reservoir 2 is 25 and it is full. Two

constraints, total flood storage capacity and reservoir storage capacity of reservoir 2, are binding in this example. Similar to the above discussion, total flood storage capacity is optimally allocated to equalize downstream peak flow (2.59) of each storm under the constrained condition.

Given a fixed incoming flood volume, the minimized maximum downstream peak flow should decrease with greater total flood storage capacity available for allocation. Comparing the optimal results in Table 4 and Table 5, when total flood storage capacity decreases from 65 to 55, maximum downstream peak flow increases from 2.06 to 2.59. In the second case, less flood volume is stored in reservoirs (there's still storage capacity left in reservoir 1) and more flood volume is released to downstream.

5.2.2 Theory and Numerical Results

As for a single flood hydrograph, ideally, available storage capacity should be allocated to provide the same marginal improvement in peak flow reduction (equalizing MFSE) for each reservoir in parallel and for each storm, so a small shift of flood storage volume from $S_{i,j}$ to $S_{i',j'}$ $\left(i' \neq i, j' \neq j\right)$ would not improve the performance of a whole system. This condition determines flood storage volumes for every storm and either parallel reservoir so that:

$$\frac{d\Delta Q_{i,j}}{dS_{i,j}} = \frac{d\Delta Q_{i',j'}}{dS_{i',j'}}, \forall i' \neq i, j' \neq j\ , \tag{36}$$

Or $$\frac{\partial \Delta Q_{i,j}}{\partial S_{i,ji}} = \frac{\partial \Delta Q_{i',j'}}{\partial S_{i',j'}} \tag{37}$$

Thus $$\frac{1}{\sqrt{{d_{i,j}}^2 + 2\alpha_{i,j}S_{i,j}}} = \frac{1}{\sqrt{{d_{i',j'}}^2 + 2\alpha_{i',j'}S_{i',j'}}} \tag{38}$$

Or $${d_{i,j}}^2 + 2\alpha_{i,j}S_{i,j} = {d_{i',j'}}^2 + 2\alpha_{i',j'}S_{i',j'} \tag{39}$$

However, if any constraint binds, $\Delta Q_{i,j}$ or $\Delta Q_{i',j'}$ could reach their limits. Then the optimal relation of $\frac{d\Delta Q_{i,j}}{dS_{i,j}} = \frac{d\Delta Q_{i',j'}}{dS_{i',j'}}$ no longer applies.

These analytical conclusions can be verified by the above optimizations. Table 6 also contains the optimal results of when total flood storage is 45 for comparison.

Table 6. Verification of numerical results

		Storm 1		Storm 2		Storm 3		Total Flood storage	
Reservoir		R1	R2	R1	R2	R1	R2	R1	R2
Total flood storage capacity is 65	Flood storage	13.18	5.24	17.90	12.48	8.91	7.27	40.00	25.00
	MFSE	0.19	0.22	0.11	0.13	0.17	0.18		
Total flood storage capacity is 55	Flood storage	10.49	5.36	12.95	12.99	6.56	6.65	30.00	25.00
	MFSE	0.22	0.21	0.13	0.13	0.19	0.19		
Total flood storage capacity is 45	Flood storage	8.28	4.94	10.61	10.92	5.08	5.16	23.97	21.03
	MFSE	0.25	0.22	0.14	0.14	0.22	0.22		

Total flood storage volume in either reservoir decreases when the total flood storage capacity decreases from 65 to 55 and further to 45. Reduced total flood storage capacity is first allocated to reservoir with smaller MFSE to increase its MFSE, according to the equalizing MFSE rule. Besides, from Table 6, MFSEs of two reservoirs for any individual storm are identical or similar, while the MFSEs among different storms differ greatly. Since the objective is to reduce the maximum downstream peak flow among all the storms, reduced downstream peak flows for each storm are as equalized as possible. In addition, total flood storage volumes of storm 1 and storm 3 are the same but less than that of storm 2. Therefore, MFSEs of storm 1 and storm 3 for all different total flood storage volumes are close but larger than those of storm 2.

5.2.3 Sensitivity Analysis of Hydrograph Shape

Similar to the discussion in 3.4.3, here sensitivity analysis is for examining the impacts on optimal flood storage volumes from hydrograph shape, which is represented by α_{ij} (rising limb and recession limb) and d_{ij} (duration of peak inflow). We can see if the above conclusion that α_{ij} has larger impacts still stands for a series of storms.

For simplification, only one parameter is used as representative for each type of hydrograph shape parameters: α_{12} and d_{12} for reservoir 1 and storm 2. Changing α_{12} and d_{12} from -50% to 50% respectively, the results are shown below. Changes of total downstream peak flow for change in α_{12} are plotted based on the left vertical axis, while the comparatively slight changes of total downstream peak flow for change in d_{12} are plotted based on the right vertical axis. Horizontal axis at 0% point is the base case.

As either parameter increases in Figure 19, the hydrograph shape becomes wider with less peak inflow or longer duration decreasing downstream peak flow. The changes of total downstream peak flow either due to α_{12} or d_{12} are of the same pattern and the optimal results are similar in Figure 18. In addition, α_{12} has larger impact than d_{12}, which conforms to the optimal results of a single storm condition.

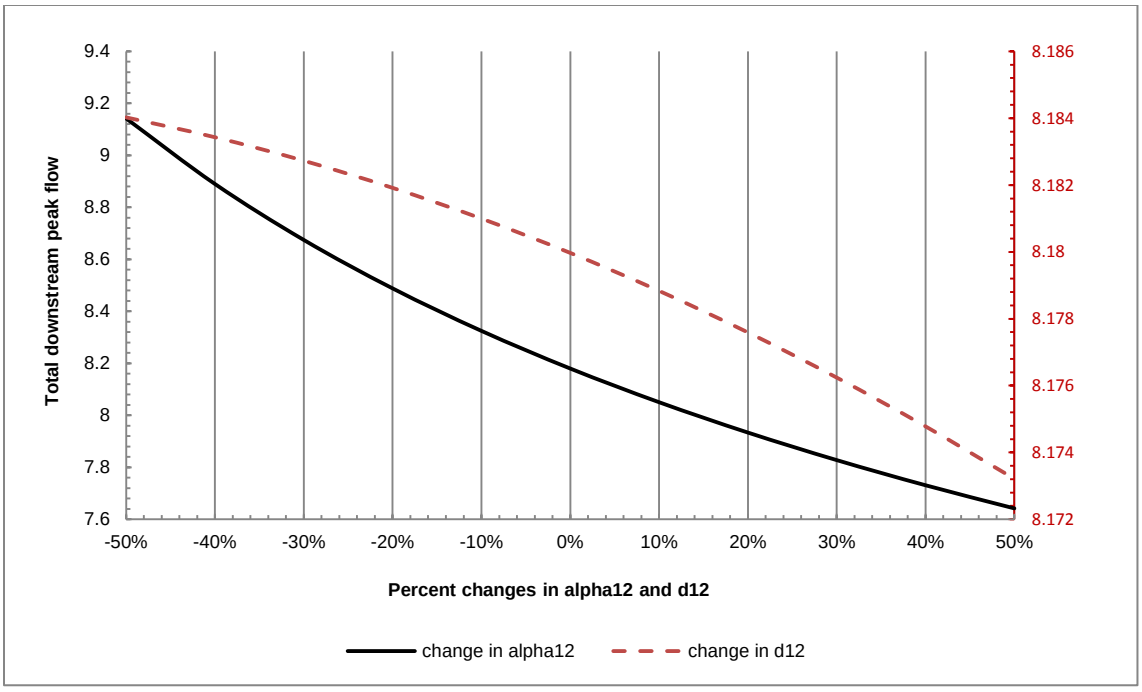

Figure 19. Impacts of hydrograph shape changes on total downstream peak flow (series of known storms model)

5.3 Series of Unknown Storms

Similar to the single storm case, for a series of storms, uncertainty still exists within each storm. So we can assume that for each storm in the predicted series, it reveals a probability distribution. Specifically, we can discretize the probability distribution to include the uncertainty of each individual storm into our optimization.

To find the ideal allocation of flood storage volumes among series of uncertain storms for the two parallel reservoirs, the following mathematical formula can be used to minimize the expected total damage of downstream peak flow:

$$Min \qquad z = \underset{j=1:l}{Max}\left[\sum_{f=1}^{m} p_{j,f} \bullet D\left(\sum_{i=1}^{n} Q_{i,j,f,outpeak}\right)\right] \tag{40}$$

Subject to:

$$\Delta Q_{ij} \le \frac{-d_{ijf} + \sqrt{d_{ijf}^{\,2} + 2\alpha_{ijf} S_{ij}^{\,0}}}{\alpha_{ijf}}, \alpha_{ijf} = \frac{a_{ijf} + b_{ijf}}{a_{ijf} b_{ijf}}, \forall f = 1, 2 \ldots m \tag{41}$$

$$\sum_{j=1}^{l}\sum_{i=1}^{n} S_{ij} \le S_{Total} \tag{42}$$

$$S_{ij}^{\,0} = S_{i,j-1}^{\,0} - S_{ij},\ j = 1, 2, \ldots l \tag{43}$$

$$Q_{ijf,outpeak} = Q_{ijf,inpeak} - \Delta Q_{ij},, \forall f = 1,2...m, \forall i, j \quad (44)$$

$$\sum_i \Delta Q_{ij} \le \sum_i Q_{ijf,inpeak} - Q_j^T, \forall f = 1,2...m \quad (45)$$

$$\Delta Q_{ij} \le Q_{ijf,inpeak}, \forall f = 1,2...m \quad (46)$$

$$\Delta Q_{ij} \ge 0 \quad (47)$$

where

$p_{j,f}$ = probability of a flood hydrograph *f* for a storm *j*

$Q_{i,j,f,inpeak}$ = peak inflow without reduction for an individual reservoir *i* and a storm *j* and a hydrograph scenario *f*

$Q_{i,j,f,outpeak}$ = peak flow after reduction for an individual reservoir *i* and a storm *j* and a hydrograph scenario *f*.

Others parameters are the same as in a series of known storms case.

So there are still $m \times n$ decision variables $\Delta Q_{ij}\left(i = 1:n,\ j = 1:m\right)$ in total in this series of uncertain storms case. However, to find the optimal results under this condition, we should use expected values to take into account the uncertainties of different hydrograph shapes.

This optimization for a series of unknown storms (Equation (40-47)) can also be solved by the non-linear Generalized Reduced Gradient method, though it might take considerable computation efforts. Furthermore, we could formulate this uncertain storm problem as a three-stage stochastic problem. The third stage would be the outcome from an actual storm given a predicted storm.

6. Case Study: Oroville Reservoir and New Bullards Bar Reservoir above Marysville

The Oroville Reservoir and New Bullards Bar Reservoir above Marysville in Sacramento River system are illustrated in Figure 20. Figure 21 shows the schematic of this simple parallel reservoir system. The total Yuba- Feather river watershed size is 6,264 square miles to the confluence with the Sutter Bypass. This includes 5,365 square miles at the Feather-Yuba confluence. The two flood control reservoirs in the system are Oroville Reservoir and New Bullards Bar Reservoir (USACE 2009).

Oroville Reservoir is formed by Oroville Dam on the Feather River, in the foothills of the Sierra Nevada about 6 miles upstream from the town of Oroville. At over 3,538,000 acre feet (4.3 km^3), it is the second largest reservoir in California, after Shasta Lake. The lake is fed by the North Fork, Middle Fork, West Branch and South Forks of the Feather River. It was built for water supply, flood control, power generation, recreation, and conservation. It includes 750,000 acre-feet of flood storage space to protect the cities of Marysville, Yuba City, Oroville and other smaller communities (USACE 1970).

New Bullards Bar Reservoir is on the Yuba River that flows into the Feather River downstream of Oroville. It was built for flood control, conservation, power generation, water supply, and recreation. It has 170,000 acre-feet of flood control storage space and a gross pool capacity of 960,000 acre-feet (USACE 1972).

Both Oroville Reservoir and New Bullards Bar Reservoir operate within flood limits defined in their water control manuals (USACE 1970, USACE 1972). These flood-related limits include: maximum downstream channel capacity at dam; maximum downstream channel capacity at various locations, including Yuba City, Marysville, and the confluence; maximum rate of flow increase; and maximum rate of flow decrease.

Descriptions of the two reservoirs are listed in Table 7.

Table 7. Reservoirs descriptions

Reservoir	Oroville[(a)]	New Bullards Bar[(b)]
Total Capacity (KAF)	3,538	966
Flood Control Space (KAF)	750	170
Standard Proj. Flood Peak Flow (cfs)	440,000	150,000
Elevation (ft)	900'	1965'
Downstream (Marysville) design Flow (cfs)[(c)]	120,000*	

(a) USACE 1970 (b) USACE 1972 (c) USACE 1993
*180,000 cfs when flows in Feather River are low

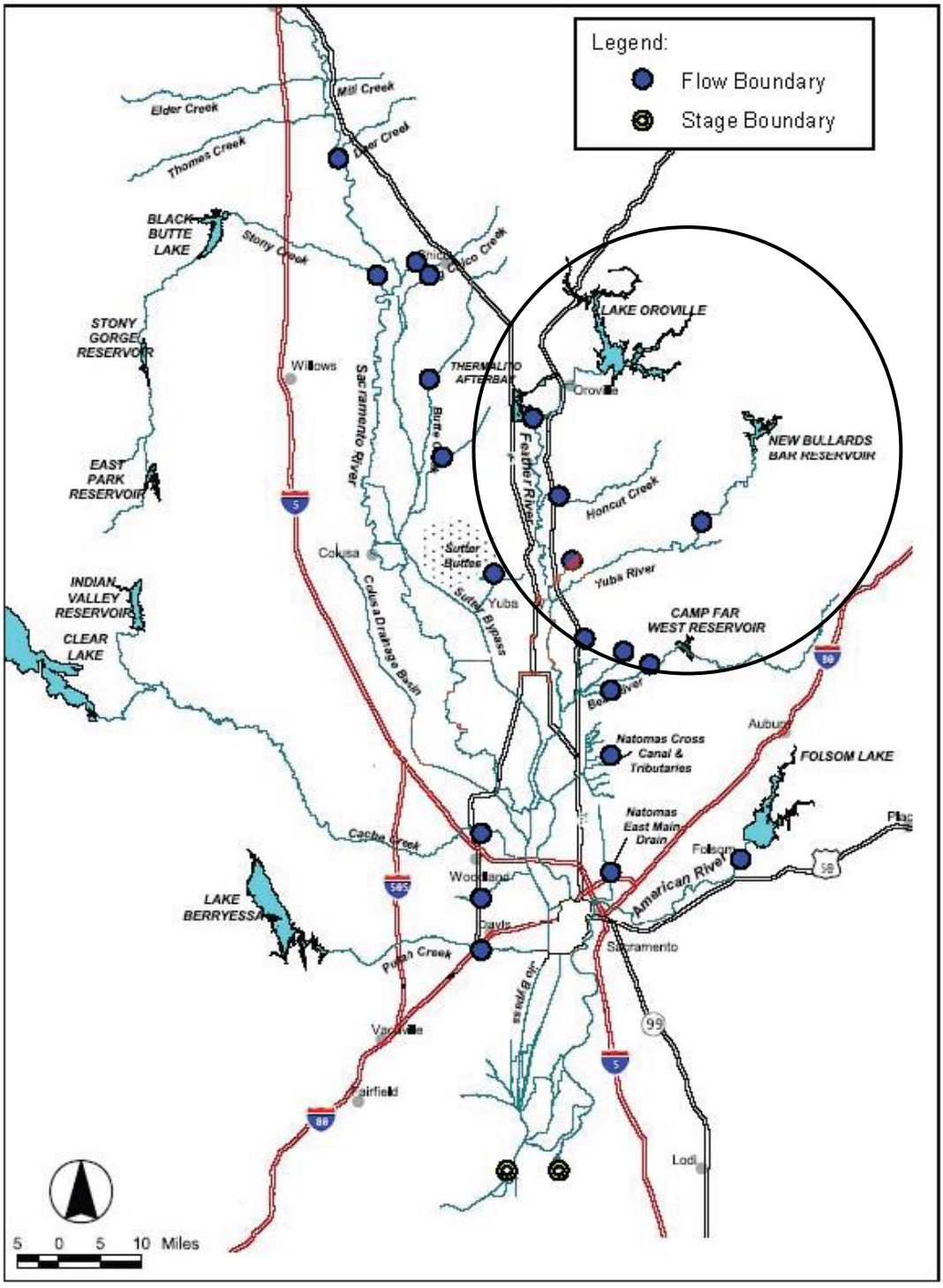

Figure 20. Oroville Reservoir and New Bullards Bar Reservoir above Marysville in Sacramento River system (Base Map by USACE)

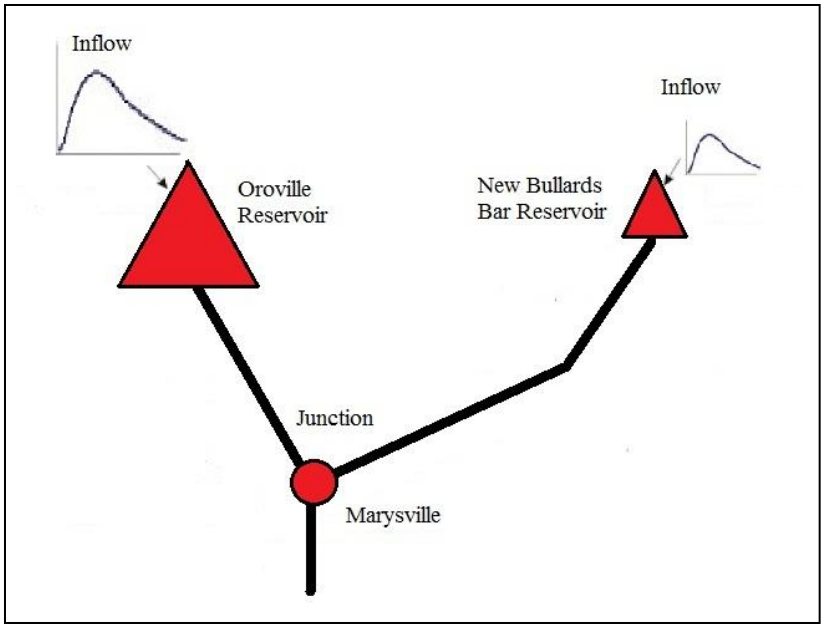

Figure 21. Schematic of Oroville Reservoir and New Bullards Bar Reservoir above Marysville

6.1 Case Study of the Simple Deterministic Allocation for a Single Known Storm

Figures in this case study are for illustrative purposes only. Data, models, and results have been simplified to illustrate key concepts related to this paper. We choose the historical 1997 flood for this simple deterministic allocation case study.

6.1.1 Historical Operation of the 1997 Storm

Figure 22 shows the 1997 flood inflow time series of Oroville Reservoir (left graph) and New Bullards Bar Reservoir (right graph). The peak inflows are 302,004 cfs for Oroville Reservoir and 104,480 cfs for New Bullards Bar Reservoir. Historically, the peak outflows were 160,917 cfs and 55,005 cfs respectively. Assuming peak outflows coincide downstream without attenuation as the release hydrograph peaks move downstream (the worst case), the downstream Marysville would have a peak flow of 216,000 cfs (the real 1997 operated downstream peak was much less due to water loss etc.). The currently allocated flood storage volumes for Oroville Reservoir and New Bullards Bar Reservoir are 659 TAF and 170 TAF respectively, totally 829 TAF. Comparing the reservoir flood control capacity and flood storage volume in two reservoirs, flood control capacity of New Bullards Bar Reservoir is fully used, while there is still flood control capacity left in Oroville Reservoir. In addition, in this parallel reservoir system, Oroville Reservoir and New Bullards Bar Reservoir account for about 80% and 20% of the summed total flood storage volume respectively. We can apply the derived optimal allocation rules to re-operate this 1997 storm to see how they work.

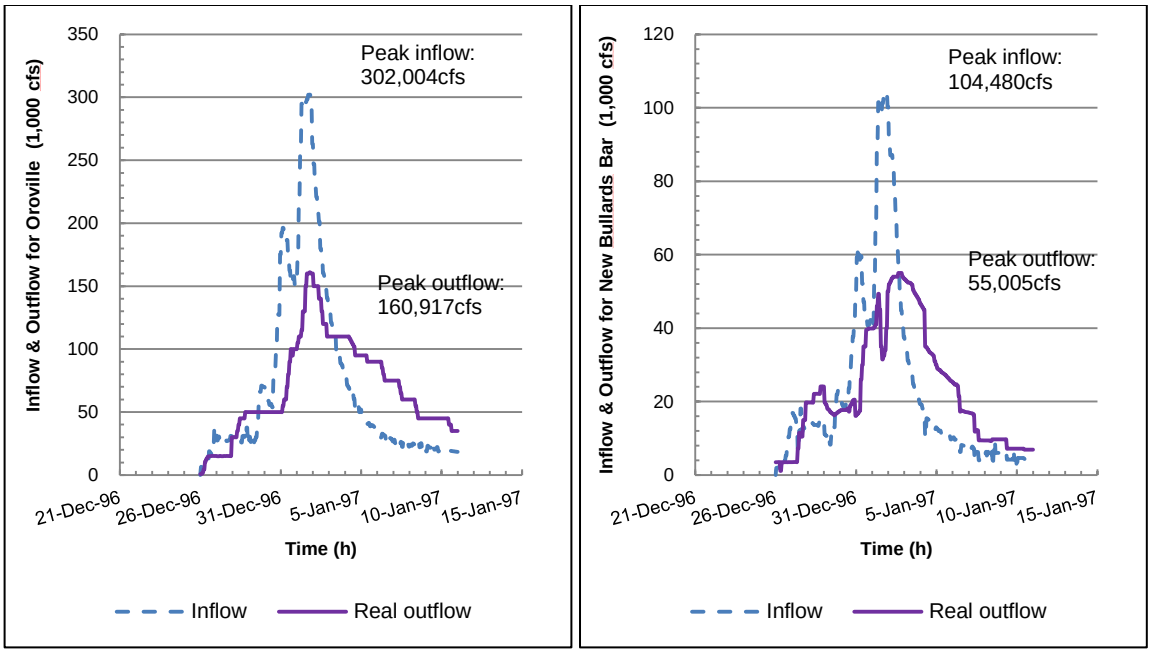

Figure 22. Historical operation of 1997 flood for Oroville Reservoir (left) and New Bullards Bar Reservoir (right)

6.1.2 Re-operation of 1997 Storm

Based on the above given data, we approximate the real 1997 hydrograph shapes of two reservoirs into the broad peak hydrograph shapes (see Figure 23).

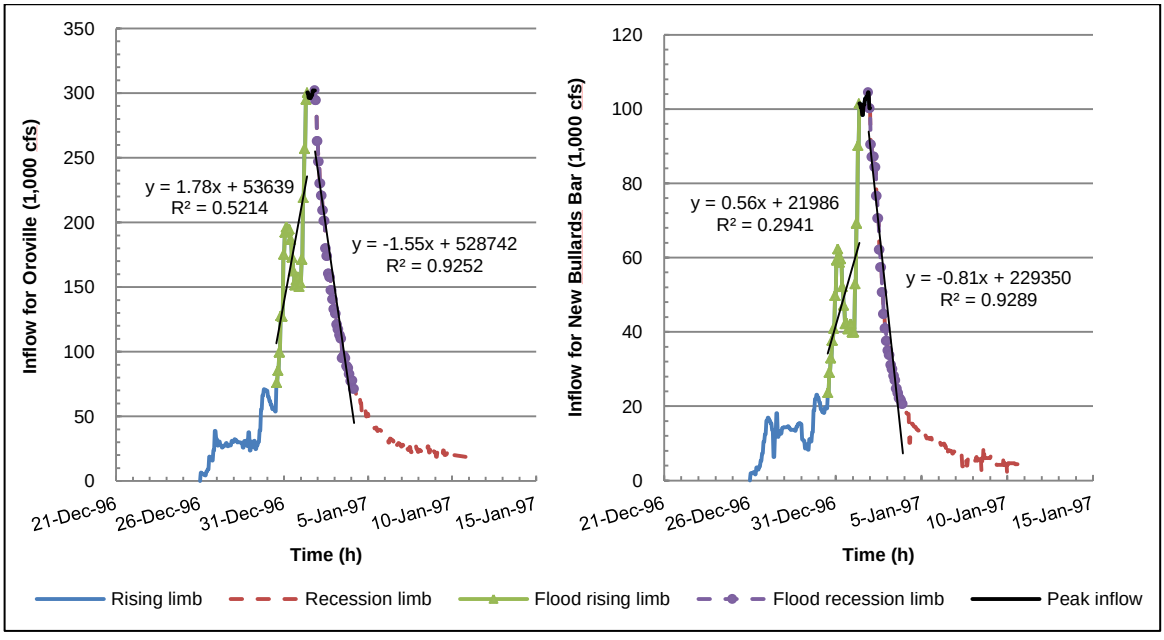

Figure 23. Approximation of 1997 flood for Oroville Reservoir (left) and New Bullards Bar Reservoir (right)

Table 8 shows hydrograph shape descriptions of Oroville and New Bullards Bar reservoirs, including designed base flow, rising and recession limbs, peak inflow, the duration of peak inflow, and incoming flood volume.

Table 8. 1997 hydrograph shape descriptions of Oroville and New Bullards Bar reservoirs

	Oroville	New Bullards Bar
Base flow (cfs)	70,000	20,000
Incoming flood volume (TAF)	942	314
Peak inflow (cfs)	302,004	104,480
Rising limb (cfs/s)	1.7800	0.5600
Recession limb (cfs/s)	1.5500	0.8100
Alpha (s/cfs)	1.2070	3.0203
Duration of peak flow (s)	39,600	50,400

Three cases are analyzed: (1) total flood storage capacity available for allocation is the same as historical 1997 flood (829 TAF); (2) total flood storage capacity available for allocation is less than historical 1997 flood (600 TAF); (3) total flood storage capacity available for allocation is still the same as historical 1997 flood (829 TAF), but the reservoir storage capacity of New Bullards Bar Reservoir increases from 170 TAF to 250 TAF. Applying the simple deterministic model into these three cases, we can derive the following results for allocating flood storage capacity among Oroville Reservoir and New Bullards Bar Reservoir.

Table 9. 1997 flood storage allocation between Oroville and New Bullards Bar reservoirs

		Oroville	New Bullards Bar
Historical allocations. Total flood storage capacity =829 TAF	Flood storage volume (TAF)	659	170
	Flood storage capacity used (%)	93	100
	Percentage of total flood storage (%)	79	21
	Peak flow reduction (cfs)	141,087	49,075
	Outflow (cfs)	160,917	55,005
	MFSE	-	-
	Downstream Peak flow (cfs)	215,922	
Case (1): Optimized allocations. Total flood storage capacity =829 TAF. Unchanged reservoir storage capacity	Flood storage volume (TAF)	659	170
	Flood storage capacity used (%)	93	100
	Percentage of total flood storage (%)	80	20
	Peak flow reduction (cfs)	187,816*	55,300*
	Outflow (cfs)	114,188*	48,780*
	MFSE	3.76e-06	4.60e-06
	Downstream Peak flow (cfs)	162,968	
Case (2): Optimized allocations. Total flood storage capacity =600 TAF. Unchanged reservoir storage capacity	Flood storage volume (TAF)	431	169
	Flood storage capacity used (%)	57	99
	Percentage of total flood storage (%)	72	28
	Peak flow reduction (cfs)	146,664	55,032
	Outflow (cfs)	155,340	49,448
	MFSE	4.62e-06	4.62e-06
	Downstream Peak flow (cfs)	204,788	
Case (3): Optimized allocations. Total flood storage capacity =829 TAF. Reservoir storage capacity of New Bullards Bar Reservoir increases from 170 to 250 TAF	Flood storage volume (TAF)	595	234
	Flood storage capacity used (%)	79	94
	Percentage of total flood storage (%)	72	28
	Peak flow reduction (cfs)	177,053	67,180
	Outflow (cfs)	124,951	36,900
	MFSE	3.95e-06	3.95e-06
	Downstream Peak flow (cfs)	161,851	

*All the peak inflows above optimal peak outflows are reduced with these parts of inflow volumes stored in reservoirs under perfect forecast condition.

First we compare the historical operation with the optimal operations in case (1) with the unchanged reservoir storage capacities and case (2) with the reduced total flood storage capacity. Then we compare the optimized allocations in case (1) and case (3) with same total flood storage capacity but different reservoir storage capacities of New Bullards Bar Reservoir.

A. Comparison of historical allocation and optimized allocations in case (1) and case (2) for 1997 flood.

In case (1) with the historical total flood storage capacity, New Bullards Bar Reservoir's storage capacity is fully used, while empty flood capacity remains for Oroville Reservoir. Comparing the flood storage volumes of each reservoir, the optimal allocations are the same as those from historical records. This is because that reservoir

storage capacity of New Bullards Bar Reservoir constrains both in historical allocation and case (1), which also leads to unequal MFSEs of the two reservoirs. With the assumption that the 1997 historical flood is perfectly known in case (1), downstream peak flow can be reduced to a lower value, cutting down all flood flows above the optimal peak flow. Yet the historical downstream peak flow has an extremely short duration. So for the same flood storage volumes, optimized downstream peak flow is much smaller than that from historical records.

If reducing total flood storage capacity from 829 TAF as in case (1) to 600 TAF as in case (2), reservoir storage capacities of two reservoirs both are not be fully used. Compared to case (1), the reduced total flood storage capacity in case (2) is almost all allocated to Oroville Reservoir to increase its relatively smaller MFSE, whereas the flood storage volume of New Bullards Bar Reservoir changes a little. Since only the total flood storage capacity constraint is binding in case (2), MFSEs of two reservoirs are ideally equal.

Optimal allocations of two different total flood storage capacities can be compared from the perspective of MFSE. When total flood storage capacity is 829 TAF, due to the reservoir storage capacity constraint of New Bullards Bar Reservoir, MFSEs of Oroville Reservoir and New Bullards Bar Reservoir are 3.76e-06 and 4.60e-06 respectively. When decreasing total flood storage capacity, the reduced storage capacity should be allocated to Oroville Reservoir first to increase its MFSE until two reservoirs have the same MFSEs. As in Table 9, the MFSEs of two reservoirs in case (2) are both 4.62e-06.

With these outcomes based on the derived flood storage capacity allocation rules, we can plot the optimal 1997 historical flood operation of Oroville and New Bullards Bar reservoirs.

Figure 24 and Figure 25 compare the two reservoirs' optimal operations of 829 TAF and 600 TAF total flood storage capacity and historical operation. For Oroville Reservoir, in case of the probable coming flood, the reservoir began to release small amount of water (772 cfs) from December 1st, 1996 on historical record. When the flood occurred, Oroville Reservoir began to release more water, and the real peak outflow far exceeds peak outflow from the optimal allocation. The results are the same for New Bullards Bar Reservoir. It also began to release water (3,488 cfs) from December 1st, 1996. Since reservoir storage capacity of New Bullard Bar Reservoir is much less than that of Oroville Reservoir, its pre-release in case of future flood is larger. Then during the flood, New Bullards Bar Reservoir released large amounts of water with bigger peak outflow than the optimal result, and changed rapidly.

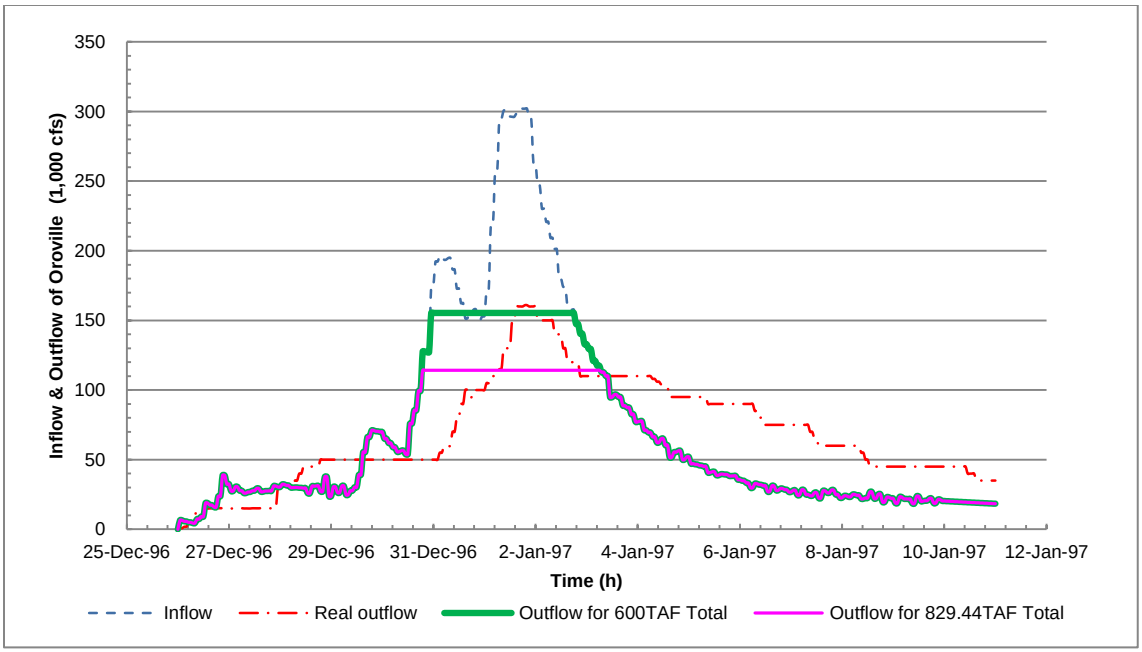

Figure 24. Optimal operation of 1997 flood for Oroville Reservoir (HEC-DSS)

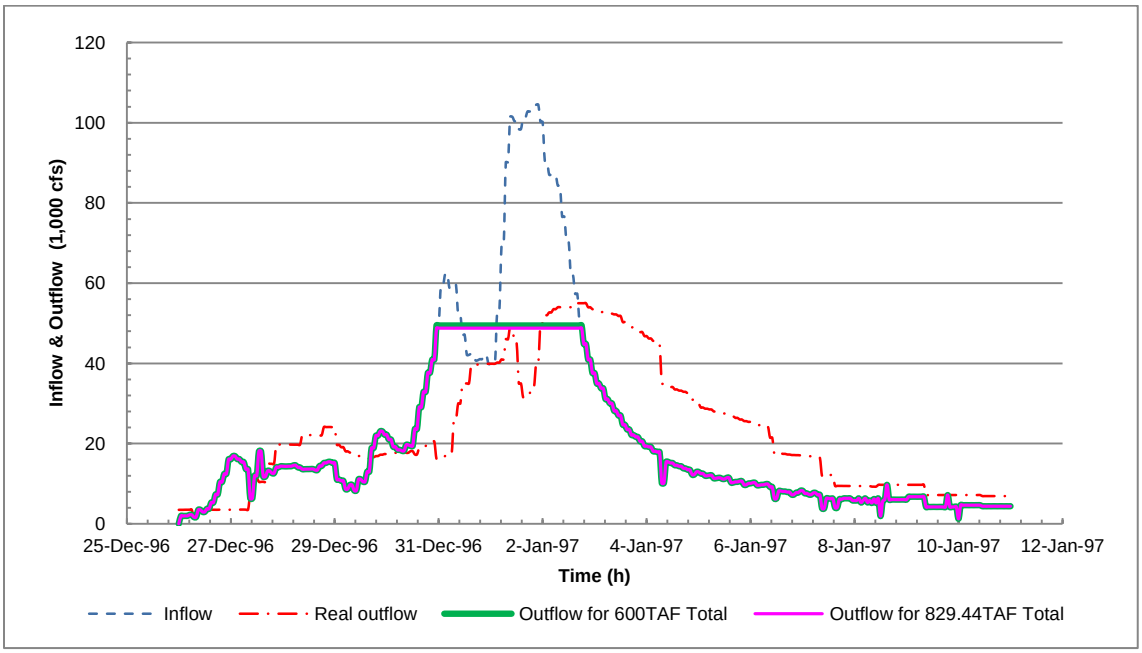

Figure 25. Optimal operation of 1997 flood for New Bullards Bar Reservoir (HEC-DSS)

The downstream (Marysville) design flow is 120,000 cfs or 180,000 cfs when Feather River flows are low (USACE 1993). So the optimal maximum downstream peak flow (162,968 cfs) may not cause damage. Figure 26 shows the downstream outflow from historical records and optimal allocations for different total flood storage capacities. Assuming no river attenuation, the 1997 maximum combined downstream peak flow is 210,005 cfs, which far exceeds the optimal result and exceeds the downstream design

flow. Therefore, there is advantage following the rising limb of the hydrograph early on.

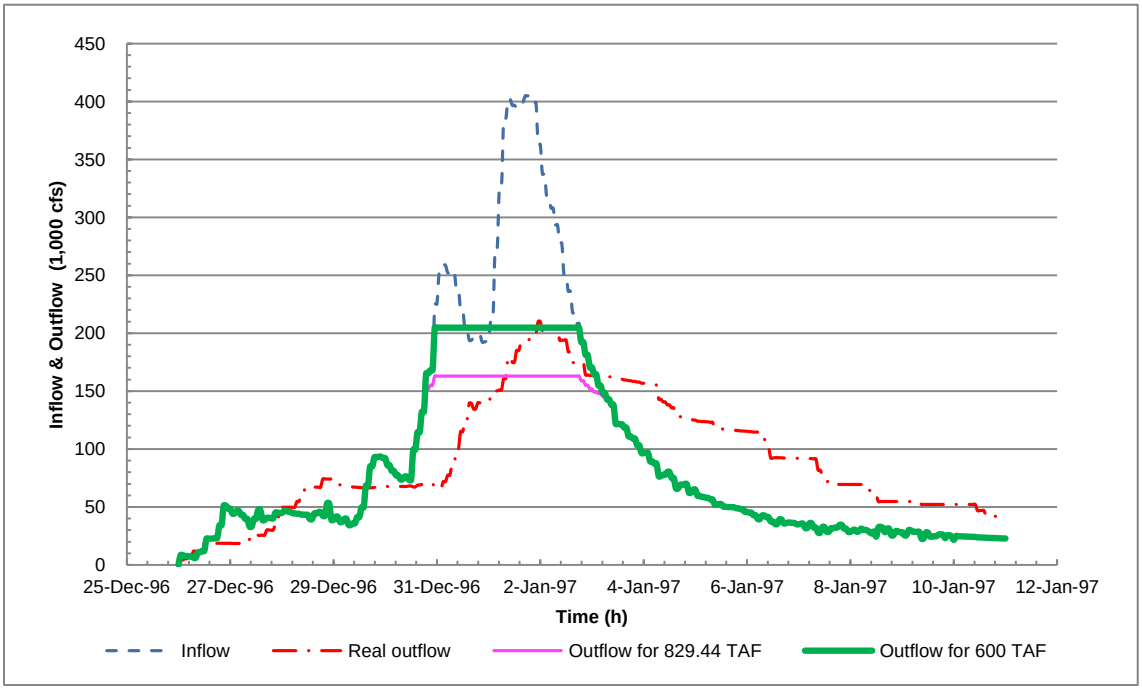

Figure 26. Optimal operation of 1997 flood for downstream (Marysville) (HEC-DSS)

From the above comparison of historical allocation and optimized allocations in case (1) and case (2), with good flood forecasts and time to balance initial storages, the optimal flood storage allocation rules can better reduce downstream peak flow through operating two parallel reservoirs based on their hydrograph shapes. Additionally, the most significant improvement from this re-operation is from improving individual performance at each reservoir, rather than improving flood storage allocation between two reservoirs.

B. Comparison of optimized allocations in case (1) and case (3) for 1997 flood.

Historical operation of the 1997 storm fully utilized the flood control capacity of New Bullards Bar Reservoir (170 TAF). Similarly, with the identical total flood storage capacity available for allocation (829 TAF) as historical operation, the re-operation of 1997 storm in case (1) is also constrained by the reservoir flood storage capacity of New Bullards Bar Reservoir. To better optimize this simple deterministic model, we can loosen this constraint by adding more reservoir storage capacity.

If we use more than the flood control capacity of New Bullards Bar Reservoir, for example storing flood volume to the top of the dam or emptying some of the conservation pool before a flood, we can increase the reservoir storage capacity to 250 TAF. With the same total flood storage capacity available for allocation, we can see how downstream damage is affected. Case (3) is the optimal allocation from re-operation of the 1997 storm with the increased 250 TAF reservoir storage capacity of New Bullards Bar Reservoir, allocating the same total flood storage capacity (829 TAF) as historical operation or case (1).

From the optimized allocations in case (1) and case (3) in Table 9, in terms of downstream peak flow, the optimal allocations of the unchanged and increased reservoir storage capacity come up with similar results. Increasing reservoir storage capacity of

New Bullards Bar Reservoir to loosen this constraint only reduces the downstream peak flow by less than 1%. Though flood storage volume transfers from Oroville Reservoir to New Bullards Bar Reservoir to optimally equalize the MFSEs of two reservoirs (both are 3.95e-06), peak flow reductions vary only a little since the flood inflow for Oroville Reservoir is comparatively large. In this case, increasing reservoir storage capacity of New Bullards Bar reservoir is not worthwhile. Additionally, for this specific 1997 storm with largely diverged storm sizes and reservoir storage capacities for two parallel reservoirs, there is a wide range of near-optimal allocations.

6.2 Case Study of an Uncertain Storm

To create a more interesting and stressful example illustrating optimal allocation with an uncertain storm, four historical and synthetic storms are used to illustrate the effort for an uncertain storm. The four possible storm hydrographs are:

(1) A small 1995 storm with a big probability of 0.85;
(2) A scaled-down 1997 storm (20% smaller for Oroville reservoir and 10% smaller for New Bullards Bar reservoir) with a probability of 0.10;
(3) A significant 1997 storm with a probability of 0.04;
(4) A scaled-up 1997 storm (20% larger for Oroville reservoir and 40% larger for New Bullards Bar reservoir) with a probability of 0.01.

Detailed input inflow data of the four storms are in Table 10.

Table 10. Hydrograph shape descriptions of two reservoirs and an uncertain storm with probabilistic hydrograph

	Proba-bility	Reservoir	Base flow (cfs)	Incoming flood volume (TAF)	Peak inflow (cfs)	Rising limb	Recession limb	Alpha	Duration of peak flow (s)
Weighted average		Oroville	70,000	285	158,078	0.84	1.35	1.94	48,067
		New Bullards Bar	20,000	70	45,294	0.27	0.51	5.64	34,798
1995 Storm	0.85	Oroville	70,000	204	139,075	0.67	1.31	2.26	50,400
		New Bullards Bar	20,000	31	35,655	0.22	0.46	6.72	32,400
Scaled-down 1997 Storm	0.1	Oroville	70,000	603	241,603	1.78	1.55	1.21	31,680
		New Bullards Bar	20,000	255	93,672	0.56	0.81	3.02	45,360
1997 Storm	0.04	Oroville	70,000	942	302,004	1.78	1.55	1.21	39,600
		New Bullards Bar	20,000	314	104,080	0.56	0.81	3.02	50,400
Scaled-up 1997 Storm	0.01	Oroville	70,000	1356	362,405	1.78	1.55	1.21	47,520
		New Bullards Bar	20,000	616	145,712	0.56	0.81	3.02	70,560

Based on our discussion in 4.2, when the sizes and probabilities of forecasted

uncertain hydrographs are distributed in broad ranges, the Two-stage Forecast method is more applicable for minimizing downstream peak flow. So given these input data, we optimize the uncertain storm by the Two-stage Forecast method. Deterministic Expected Forecast method is also used for comparison.

6.2.1 Optimal Operation of an Uncertain Storm with Designed Reservoir Capacities

Here individual reservoir storage capacity is still 750 TAF for Oroville Reservoir and 170 TAF for New Bullards Bar Reservoir (designed reservoir flood control capacities). Total flood storage capacity available for allocation is assumed to be 200 TAF. Optimal results are shown in Table 11 from both the Two-stage Forecast method and the Deterministic Expected Forecast method.

Table 11. Optimal storage allocations from Deterministic Expected Forecast and the Two-stage Forecast methods of four probable hydrographs for Oroville and New Bullards Bar reservoirs.

		Reservoir	Flood storage (TAF)	Peak flow reduction (cfs)	MFSE (e-05)	Outflow (cfs)	Downstream peak flow (cfs)
Deterministic Expected Forecast [a]		Oroville	147	60,233	0.607	97,845	**120,091 (203,372)***
		New Bullards Bar	53	23,049	0.607	22,245	
Two-stage Forecast [b]		Oroville	159	61,582	2.12	96,496	**126,135 (203,372)***
		New Bullards Bar	30	15,655	2.94	29,639	
Second stage performance of the Two-stage Forecast [c]	1995 Storm	Oroville	169	61,582	1.98	77,493	**97,493 (174,730)***
		New Bullards Bar	31	15,655	3.09	20,000	
	Scaled-down 1997 Storm	Oroville	97	61,582	3.16	180,021	**258,038 (335,275)***
		New Bullards Bar	25	15,655	2.20	78,017	
	1997 Storm	Oroville	109	61,582	2.53	240,422	**328,847 (406,084)***
		New Bullards Bar	27	15,655	1.98	88,425	
	Scaled-up 1997 Storm	Oroville	120	61,582	2.10	300,822	**430,879 (508,117)***
		New Bullards Bar	34	15,655	1.42	130,057	

*Simulated unmanaged downstream peak flows without river attenuation.
(a) Optimization with Deterministic Expected Forecast method using the expected hydrograph as input data.
(b) Optimization with Two-stage method applying identical decision variables to each uncertain hydrograph and minimizing the expected outcomes.
(c) Individual performance of Two-stage method with the applied identical decision variables.

From Table 11, optimal results from the Deterministic Expected Forecast are only constrained by total flood storage capacity, while those from the Two-stage Forecast method are constrained by total flood storage capacity and flood volume (maximum peak flow reduction) of New Bullards Bar Reservoir. Peak flow reductions of Oroville Reservoir are similar from both methods, whereas those of New Bullards Bar Reservoir differ greatly. The reason is that peak inflow of New Bullards Bar Reservoir of the 1995 storm is very small, and the Two-stage Forecast optimization is constrained for all the individual hydrographs. However, the expected peak inflow of New Bullards Bar Reservoir taken as input for the Deterministic Expected Forecast optimization is larger, so the peak inflow of New Bullards Bar Reservoir of the 1995 storm constraint does not bind in the Deterministic Expected Forecast optimization. Also, the MFSEs of Oroville and New Bullards Bar reservoirs from the Deterministic Expected Forecast are identical, while those from the Two-stage Forecast differ slightly. In addition, minimized downstream peak flows from the two methods are similar.

However, if the far smaller storm happens, optimal allocation from the Deterministic Expected Forecast method might no longer satisfy the flood volume constraints. For example, when the 1995 storm occurs, optimal outflow of New Bullards Bar Reservoir from the Deterministic Expected Forecast would be below the base flow. This situation can worsen for far smaller storms, under which condition optimal outflow may be larger than inflow. With respect to the Two-stage Forecast optimization, optimal allocation satisfies each individual hydrograph so it remains valid for all storms.

6.2.2 Optimal Operation of an Uncertain Storm with Reservoir Capacities in 2012

To illustrate the practical application of these optimizations, we can optimize with the recent reservoir storage on November 18, 2012 assuming that the uncertain storm in Table 10 will happen. Table 12 shows the optimal allocations from the Deterministic Expected Forecast method and the Two-stage Forecast method.

Individual reservoir storage on Nov. 18, 2012 is 1,778 TAF for Oroville Reservoir and 571 TAF for New Bullards Bar Reservoir. So the available reservoir storage capacities are 908 TAF for Oroville Reservoir and 155 TAF for New Bullards Bar Reservoir. By replacing the previous reservoir storage capacities (750 TAF for Oroville Reservoir and 170 TAF for New Bullards Bar Reservoir) with current values and assuming that reservoir storage capacities can be entirely used, the current total flood storage capacity available for allocation is 1,063 TAF (the sum of two current storage capacities). This assumes enough operational and release capability to rebalance storage in the two reservoirs before the onset of the storm.

Table 12. Optimal storage allocations from the Deterministic Expected Forecast and the Two-stage Forecast methods of four probable hydrographs for Oroville Reservoir and New Bullards Bar Reservoir system (recent reservoir capacities in 2012)

		Reservoir	Flood storage (TAF)	Peak flow reduction (cfs)	MFSE (e-05)	Outflow (cfs)	Downstream peak flow (cfs)
Deterministic Expected Forecast		Oroville	270	88,078	0.457	70,000	**90,000 (203,372)***
		New Bullards Bar	62	25,294	0.563	20,000	
Two-stage Forecast		Oroville	191	69,075	2.12	89,003	**118,643 (203,372)***
		New Bullards Bar	30	15,655	2.94	29,639	
Second stage performance of the Two-stage Forecast	1995 Storm	Oroville	203	69,075	1.98	70,000	**90,000 (174,730)***
		New Bullards Bar	31	15,655	3.09	20,000	
	Scaled-down 1997 Storm	Oroville	116	69,075	3.16	172,528	**250,545 (335,275)***
		New Bullards Bar	25	15,655	2.20	78,017	
	1997 Storm	Oroville	129	69,075	2.53	232,929	**321,354 (406,084)***
		New Bullards Bar	27	15,655	1.98	88,425	
	Scaled-up 1997 Storm	Oroville	141	69,075	2.10	293,330	**423,387 (508,117)***
		New Bullards Bar	34	15,655	1.42	130,057	

*Simulated unmanaged downstream peak flows without river attenuation.

In Table 12, optimal allocations from both the Deterministic Expected Forecast and the Two-stage Forecast optimizations are constrained by the flood volumes of Oroville and New Bullards Bar reservoirs. For the Deterministic Expected Forecast optimization, the binding flood volumes are the expected value of all hydrographs that balance the largely differed storm sizes, yet the extremely smaller flood volumes of the smallest 1995 storm are binding for the Two-stage Forecast optimization. Therefore peak flow reductions of both Oroville and New Bullards Bar reservoirs differ between these two methods. Besides, the MFSEs of Oroville and New Bullards Bar reservoirs differ from two methods. In terms of reducing downstream peak flow, optimal results from the Deterministic Expected Forecast are better. However, the same problem exists as in Table 11. When the 1995 storm occurs, peak flow reduction from the Deterministic Expected Forecast exceeds the inflow. So the allocation from the Deterministic Expected Forecast is often not optimal.

Comparing the results from the Two-stage Forecast method in Table 12 and Table 11, because of the same binding flood volume constraints of New Bullards Bar Reservoir of the 1995 storm, optimal peak flow reductions for New Bullards Bar Reservoir are both 15,655 cfs. Total flood storage capacity is binding on optimal allocation in Table 11, but not in Table 13. However, the peak flow reduction constraint of the 1995 storm binds on Oroville Reservoir in Table 13. Comparing the results from the Deterministic Expected Forecast in Table 12 and Table 11, instead of the total flood storage volume constraint in Table 11, peak flow reduction constraints of the two reservoirs bind the optimal allocation in Table 12. So more flood volume is stored in both reservoirs and MFSEs of both

reservoirs decrease with a slight difference.

To illustrate the even worse consequence that the optimized outflow from the Deterministic Expected Forecast method might be bigger than inflow, we can re-optimize the above example of current reservoir capacities situation by exchanging the probabilities of the 1995 storm and 1997 storm. Under this condition, we have a significant 1997 storm with the biggest probability (0.85) and a small 1995 storm with a tiny probability (0.04), and two other unchanged scale-down and scale-up 1997 storms as well. Since the optimal allocation from the Two-stage Forecast optimization is constrained by the peak inflows of the 1995 storm for both reservoirs, varying probabilities of different hydrograph scenarios do not change this allocation. For the Deterministic Expected Forecast method, input data are directly affected by the probability distribution so that optimal allocation changes significantly. The updated input data and optimal allocation from Deterministic Expected Forecast method are summarized in Table 13.

Table 13. Optimal storage allocations from Deterministic Expected Forecast method of probable hydrograph scenarios for Oroville Reservoir and New Bullards Bar Reservoir system (unrealistic)

Reservoir	Oroville	New Bullards Bar
Base flow (cfs)	70,000	20,000
Incoming flood volume (TAF)	883	300
Peak inflow (cfs)	290,051	100,719
Rising limb	1.7356	0.5464
Recession limb	1.5404	0.796
Alpha	1.22	3.09
Duration of peak flow (s)	39,319	49,378
Flood storage (TAF)	883	155
Peak flow reduction (cfs)	220,051	52,153
MFSE	3.24e-06	4.75e-06
Outflow (cfs)	70,000	48,565
Downstream peak flow (cfs)	118,565	

In this example, expected incoming floods for both reservoirs are dominated by the large storm with the biggest probability. The optimal allocation in Table 13 stores all incoming flood volume for Oroville Reservoir and fully uses the storage capacity of New Bullards Bar Reservoir. Remaining flood volume of New Bullards Bar Reservoir is released to downstream. Since the uncertain storm are not ideally operated, MFSEs of two reservoirs differ. Similar to but worse than the operation in Table 12, this seemingly optimal allocation isn't applicable for the smallest 1995 storm alone. Peak inflows in 1995 storm are 139,075 cfs for Oroville Reservoir and 35,655 cfs for New Bullards Bar Reservoir, both are much smaller than the corresponding optimal peak flow reductions. So these results are no longer optimal. In terms of this issue, the Two-stage Forecast optimization is more applicable when there are big differences among the sizes and probabilities of forecasted uncertain hydrographs.

In summary, the derived optimal allocation rules perform well for the historical 1997 flood as a simple deterministic storm model. The equalizing MFSE rules are proven again: additional flood storage capacity will be allocated to reservoir with greater MFSE. And the improvement from re-operation of the 1997 flood is from improving the single

reservoir performance rather than improving the flood storage allocation between two reservoirs. Specifically, increasing reservoir storage capacity of New Bullards Bar reservoir is not worthwhile since two flood inflows differ significantly. For the uncertain storm case, optimal allocations from the Two-stage Forecast method are more applicable given broadly distributed forecasted hydrographs.

7. Conclusions

For a parallel reservoir system, flood flows from upstream usually should be regulated together to reduce downstream peak flows. This typically involves allocating total flood storage capacity between parallel reservoirs.

To investigate the impacts of hydrograph shapes on flood storage allocation for two parallel reservoirs, we define the *Flood Storage Efficiency* (FSE) as the peak reduction per unit storage, and its derivate, *Marginal Flood Storage Efficiency* (MFSE).

The ideal unconstrained allocation of total flood storage capacity is for parallel reservoirs to have the same MFSEs, regardless of the flood storage capacities or the incoming flood volumes. Examples show the effects from both constraints and hydrographs under typical conditions. Relative Hydrograph Shape at an equal 50% storage allocation RHS_{50}, or the ratio of median MFSEs of two hydrograph shapes, changes optimal flood storage allocations. Hydrograph shape combinations that contain flood pulse hydrographs differ from the others. For constant flood volume, flood storage capacity allocation only depends on relative hydrograph shape, unless constraints bind.

For cases of an uncertain storm, and series of known and unknown storms, the optimal allocation rules are the same as those derived from the simple deterministic model. Specifically, ideal optimal operations equalize MFSEs of both reservoirs and all individual storms. However, optimal MFSEs are always approximately equal as more constraints added. Additionally, appropriate methods should be used for different uncertain storms. For example, the Deterministic Expected Forecast and the Expected Perfect Forecast methods are more effective for more certain forecasted storms to minimize downstream peak flow and equalize MFSEs. Whereas the Two-stage Forecast optimization is more suitable when there are big differences among the sizes and probabilities of forecasted uncertain storms.

These derived optimal flood storage capacity allocation rules are applied to Oroville Reservoir and New Bullards Bar Reservoir above Marysville in Sacramento River system for both the single deterministic storm case and an uncertain storm case. For the historical 1997 storm as a deterministic storm, the derived optimal allocation rules work well. The equalizing MFSE rules are again proven by the comparisons of historical operation and optimal operations: additional increased (reduced) total flood storage will be allocated to the reservoir with bigger (smaller) MFSE. Improving the single reservoir performance rather than improving the flood storage allocation between two reservoirs leads to the improvement of re-operation of the 1997 storm. What's more, re-operation of the 1997 storm with increased New Bullards Bar Reservoir storage capacity is deemed to be not worthwhile. Even ideal operation can be achieved that New Bullards Bar's storage capacity is not binding and MFSEs of two reservoirs are the same, downstream peak flow slightly decreases due to the greatly diverse flood hydrographs of two reservoirs. For the synthetic broadly distributed uncertain storm case, optimization with the Two-stage Forecast optimization is applicable for both designed reservoir storage capacities and current reservoir storage capacities.

For future work, these models can be extended to include water loss along the stream and flood travel time. Also, the linear damage function can be replaced with damage functions in other forms to see their impacts on optimal allocations. Additionally, the uncertain storm case can be formed as a three-stage stochastic problem.

Reference

Chang, FJ and Chang, YT (2006) *"Adaptive neuro-fuzzy inference system for prediction of water level in reservoir"* Advances in water resources, 29(1), 1-10.

Change, LC (2008) *"Guiding rational reservoir flood operation using penalty-type genetic algorithm"* Journal of hydrology, 354(1-4), 65-74.

Cheng, CT (1999) *"Fuzzy optimal model for the flood control system of the upper and middle reaches of the Yangtze River"* Hydrologial sciences journal- Journal des sciences hydrologiques, 14(4), 573-582.

Jain, SK; Yoganarasimhan, GN; Seth, SM (1992) *"A risk-based approach fro flood-control operation of a multipurpose reservoir"* Water resources bulletin, 28(6), 1037-1043.

Kumar, DN; Baliarsingh, F and Raju, KS (2010) *"Optimal Reservoir Operation for Flood Control Using Folded Dynamic Programming"*, Water resources management, 24(6), 1045-1064.

Labadie, J. W. (2004) *"Optimal Operation of Multireservoir Systems: State-of-the-Art Review."* Journal of water resources planning and management, 130, 93-111.

Lund, J. R. and Guzman, J. (1999) *"Derived operating rules for reservoirs in series or in parallel."* Journal of water resources planning and management, 125, 143-153.

Shrestha, BP, Duckstein, L and Stakhiv, EZ (1996) *"Fuzzy rule-based modeling of reservoir operation"* Journal of water resources planning and management, 122(4), 262-269.

Wang, YC; Yoshitani, J and Fukami, K (2005) *"Stochastic multiobjective optimization of reservoirs in parallel"* Hydrological processes, 19(18), 3551-3567

United States Army Corps of Engineers (USACE), 1970. *Oroville Dam and Reservoir: Report on Reservoir Regulation for Flood Control*, U.S. Army Corps of Engineers, Sacramento, CA.

USACE, 1972. *New Bullards Bar Reservoir: Reservoir Regulation for Flood Control*, U.S. Army Corps of Engineers, Sacramento, CA.

USACE, 1993. *Hydrologic Frequency Analysis, Engineer Manual (EM)* 1110-2-1415, U.S. Army Corps of Engineers, Washington, D.C.

USACE, 1997. *Hydrologic Engineering Requirements for Reservoirs, EM* 1110-2-1420, U.S. Army Corps of Engineers, Washington, D.C.

USACE, 2009. *Appendix VI: Illustrative Example (DRAFT)*. Prepared by David Ford Consulting Engineers, Inc., Sacramento, CA.

Yazdi, J and Neyshabouri, SAAS (2012) *"Optimal design of flood-control multi-reservoir system on a watershed scale"* Natural hazards, 63(2), 629-646.

Yeh, W. W-G. (1985) "*Reservoir Management and Operations Models: A State-of-the-Art Review*" Water Resources Research, 21 (12), 1797-1818.